[PS]Petroleum Charge Analysis of the Southern San Joaquin Basin, California: Implications for Future Exploration*

Alton A. Brown[1]

Search and Discovery Article #30665 (2020)**
Posted July 6, 2020

*Adapted from poster presentation given at 2002 AAPG Annual Convention and Exhibition, Houston, Texas, March 10-13, 2002
 DOI:10.1306/30665Brown2020

[1]Consultant, Richardson, Texas (altonabrown@yahoo.com)

Abstract

Southern San Joaquin Basin petroleum charge was analyzed to evaluate basin prospectivity in areas with low exploration success. Cuttings data were used to map SPI and to calibrate transformation. Petroleum generation was calculated from SPI and transformation maps. Migration was evaluated using structural configuration and stratigraphic focusing. Petroleum charge was then compared to oil-in-place and leakage to determine areas with significant charge, but little discovered petroleum. Generation from Tertiary source rocks is restricted to the Maricopa subbasin, Buttonwillow depocenter, Valley Syncline and Avenal Syncline. All significant petroleum accumulations are located where focused charge from these areas is probable.

Oil generation is Pliocene to Recent, with mostly Pleistocene generation. Tertiary source rocks in the deepest parts of the basin are barely in the gas window. Structural noses shield the east-central part of the basin from most charge and focus this oil towards the Bakersfield nose and Helm Field area. Generation occurs east of these barriers, but structural traps are absent and stratigraphic trapping is rare due to unfavorable orientation of known sandstone pinchouts. Essentially no Tertiary oil was generated in the western disturbed belt, so charge to the western part of the disturbed belt requires an older (Cretaceous?) source rock or a migration pathway from the east destroyed by subsequent deformation. Unassociated thermogenic gas potential is limited to the deepest parts of the basin by thermal maturity. Deep-basin oil potential is limited to fractured reservoirs because deeply buried sandstones have matrix permeability too low for economic oil production rates.

PETROLEUM CHARGE ANALYSIS OF THE SOUTHERN SAN JOAQUIN BASIN, CALIFORNIA: IMPLICATIONS FOR FUTURE EXPLORATION

Alton A. Brown, Consultant, Richardson, TX, altonabrown@yahoo.com

ABSTRACT

Southern San Joaquin basin petroleum charge was analyzed to evaluate basin prospectivity in areas with low exploration success. Cuttings data were used to map SPI and to calibrate transformation. Petroleum generation was calculated from SPI and transformation maps. Migration was evaluated using structural configuration and stratigraphic focusing. Petroleum charge was then compared to oil-in-place and leakage to determine areas with significant charge, but little discovered petroleum. Generation from Tertiary source rocks is restricted to the Maricopa subbasin, Buttonwillow depocenter, Valley Syncline and Avenal Syncline. All significant petroleum accumulations are located where focused charge from these areas is probable. Oil generation is Pliocene to recent, with mostly Pleistocene generation. Tertiary source rocks in the deepest parts of the basin are barely in the gas window.

Structural noses shield the east-central part of the basin from most charge and focus this oil towards the Bakersfield nose and Helm field area. Generation occurs east of these barriers, but structural traps are absent and stratigraphic trapping is rare due to unfavorable orientation of known sandstone pinchouts. Essentially no Tertiary oil was generated in the western disturbed belt, so charge to the western part of the disturbed belt requires an older (Cretaceous?) source rock or a migration pathway from the east destroyed by subsequent deformation. Unassociated thermogenic gas potential is limited to the deepest parts of the basin by thermal maturity. Deep-basin oil potential is limited to fractured reservoirs, because deeply buried sandstones have matrix permeability too low for economic oil production rates.

Approaches to Basin-Scale Exploration Evaluation

Future discoveries in a basin are traditionally evaluated from statistical analysis of drilling history, discovery history, and field size distribution (e. g., Drew and Schuenemeyer, 1993). In cases where remaining resources are estimated, the technology does not provide a methodology of how to find these resources.

An alternate approach is charge analysis (Bishop et al., 1983). Charge analysis evaluates the amount of petroleum generated in an area and the factors controlling efficiency and direction of petroleum migration and trapping. In most settings, secondary migration efficiency is so poorly constrained that resource prediction is qualitative. However, the charge analysis approach can identify weaknesses in the petroleum system so that exploration effort can be focused on locating the critical elements missing from the basin as a whole.

This study is a test of the charge analysis approach on a basin which is mature in many areas yet is sparsely drilled in deeps and marginal areas with modest deformation. Mature parts of the basin provide local calibration for charge controls on trapping in sparsely explored parts of the basin.

Stratigraphic Framework

Southern San Joaquin Tertiary strata were subdivided into 6 stratigraphic units for source rock evaluation (boundaries indicated by red lines). The boundaries approximate time lines, but shift to follow major lithostratigraphic boundaries for ease of compilation of cuttings data. The lithostratigraphic units are named after their approximate age. The Plio-Pleistocene lacks source potential, and the Eocene unit lacks source potential below the Kreyenhagen Fm. Data were not available for Cretaceous source rocks. Cretaceous source rocks are apparently restricted to the northern part of the study area.

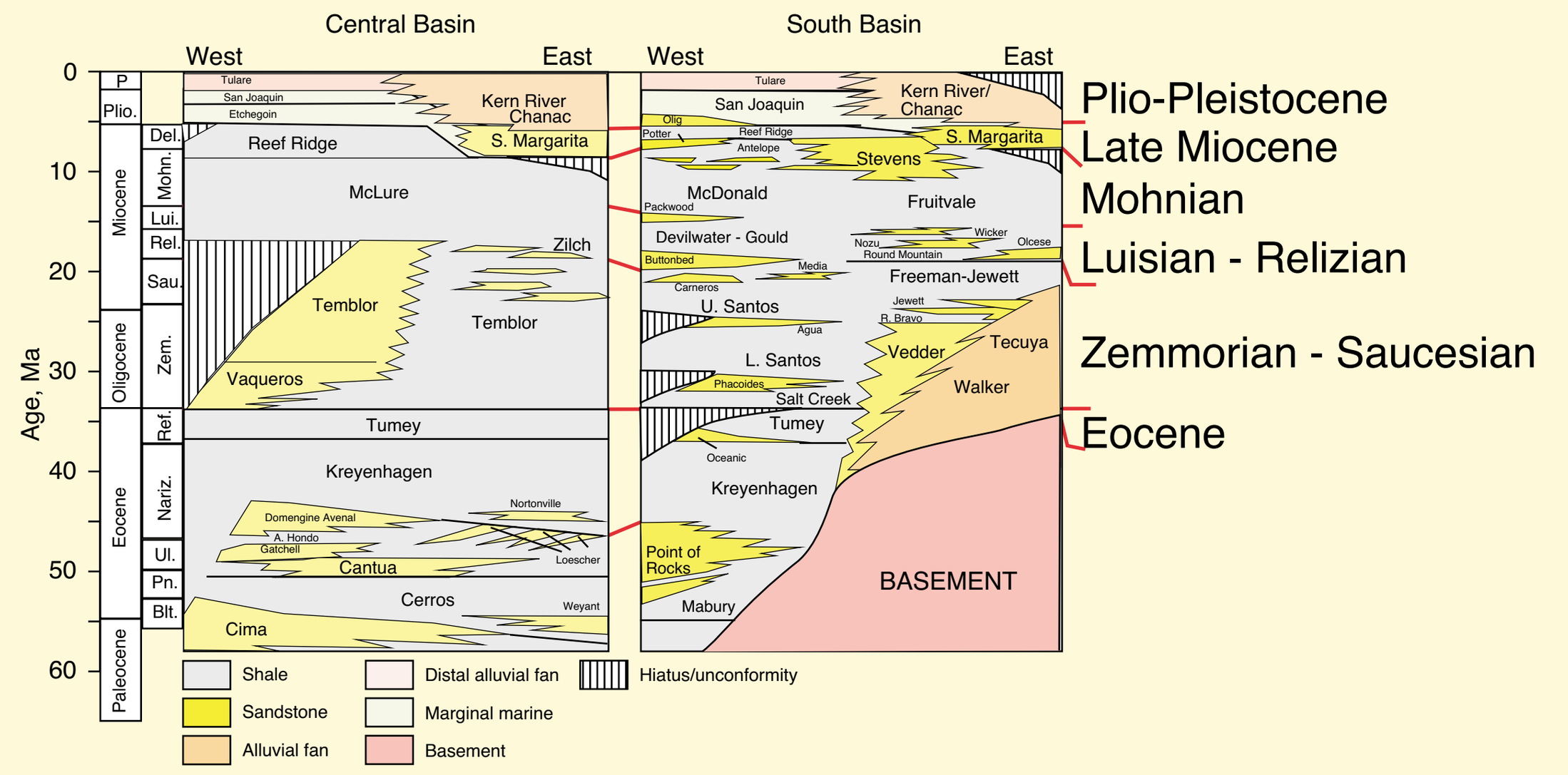

Figure greatly modified from Callaway and Rennie (1991), incorporating age and depositional data from Callaway (1990). Ages are from 1999 GSA time scale.

Oil Families and Petroleum Systems

Geochemical studies have typed southern San Joaquin oils to three source rocks: Miocene-aged source rocks, Eocene (mainly the Kreyenhagen Formation) source rock and Cretaceous (Moreno) source rock (Peters, et al., 1994; Davis et al., 1996). Isotopically heavy, Early Miocene oils similar to those of the Cuyama basin (Lundell and Gordon 1988) have not been identified in the southern San Joaquin basin, although some Early Miocene shales have source-quality kerogen and adequate thermal alteration for generation.

Petroleum Systems

Petroleum systems are identified on the basis of regional seals which constrain migration (Brown 1994). Systems mix where seals are ineffective at the basin margins.

Five petroleum systems are identified in the southern San Joaquin basin:

(1): Pliocene bacterial gas

The basal seal comprises the Reef Ridge and Macoma shales, which limits the system to the basin center. Interbedded sands and shales and broad gathering areas allow formation of large accumulations. The system is breached at several locations near the western disturbed zone. Dry gas is bacterial in origin (Kamerling, et al.1989). This system was not analyzed.

(2) Upper Miocene system

Basal seals are Round Mountain and equivalent shales in the basin center and Fruitvale shale updip on the east side. Source rocks are Miocene. Major reservoirs are Stevens, Chanac, Santa Margarita, and fractured shales. In the northern basin, the McLure shale is the basal seal and the system is uncharged due to immaturity. Basal seals are absent along the extreme east margin and in parts of the western disturbed zone, so the system mixes with the underlying system.

(3) Temblor System

Basal seals are the Santos and equivalent shale in the southern basin center and Tumey-Kreyenhagen Shale farther north. Reservoirs are mostly absent or poorly developed in the basin center. The system becomes geopressured in this area. The system merges with the Eocene system in the southernmost basin where seals are absent. Source rocks are Miocene with small mixtures of Eocene in the southern basin and predominantly Eocene with a small mixture of Miocene oils in the northern basin.

(4) Eocene System

Basal seals are not known in the southern basin. Major reservoirs are the Phacoides, Oceanic, and Point of Rocks sandstones. Tumey- Kreyenhagen is not an effective top seal in the southern part of the basin due to Oligocene tectonic disruption. Eocene source rocks are marginal to the east.

In the north, Cretaceous shales form the basal seal, and Kreyenhagen seals are disrupted only over major structures and along the western disturbed zone. The Gatchell, McAdams, and Cantua Sandstones are the main carrier beds. Oils are predominantly Eocene-sourced (Peters et al., 1994) with possible contribution from the Cretaceous system that underlies the Eocene system in the northern basin.

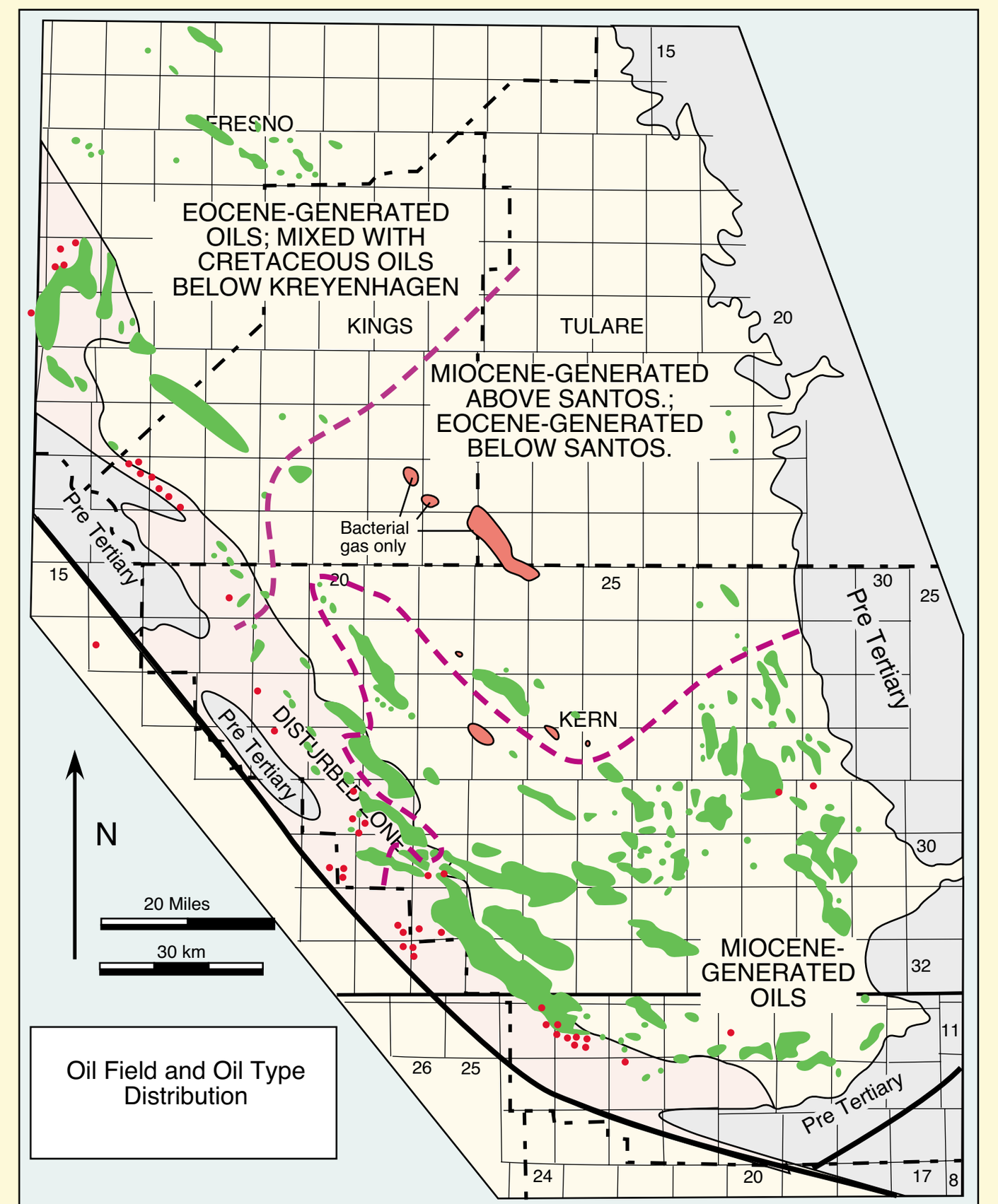

Field distribution from California Division of Oil and Gas (1985); seeps (red dots) from Hodgson (1980). Oil type distribution from published and proprietary sources.

Charge Analysis Methodology

Charge analysis has three steps: (1) estimate generation from the quantity and thermal maturity of the source rocks, (2) evaluate controls on migration efficiency and direction, and (3) evaluate types and weaknesses of potential traps. (1) Generation will be estimated from source potential Index (SPI) and transformation ratio (TR) maps. The products are maps of petroleum generation per unit area. (2) Expulsion efficiency is estimated as a function of TR and hydrogen index (HI). Secondary migration direction is controlled by structural configuration with local stratigraphic complications. Burial history modeling is used to constrain timing and choice of suitable structure configuration controlling migration. Secondary migration efficiency is empirically estimated by comparing charge with reserves in well explored areas. (3) Trap weaknesses and types are evaluated from the overall stratigraphic, tectonic, and diagenetic framework of the basin along with evaluation of analog traps.

Source Rock Distribution and SPI

SPI maps were constructed from cuttings pyrolysis data and stratigraphic interval isopachs. Cuttings data were subdivided into the 6 stratigraphic intervals. Within each interval, zones with S_2 greater than 2 mg/kg pyrolysis yield were identified. The average S_2, net thickness of the source zones, and rock density (2.6 g/cc) were multiplied to give the SPI in metric tonnes per square meter. S_2 values were corrected for transformation where they were in the oil window. SPI values were contoured by hand to incorporate reported facies changes for the stratigraphic interval.

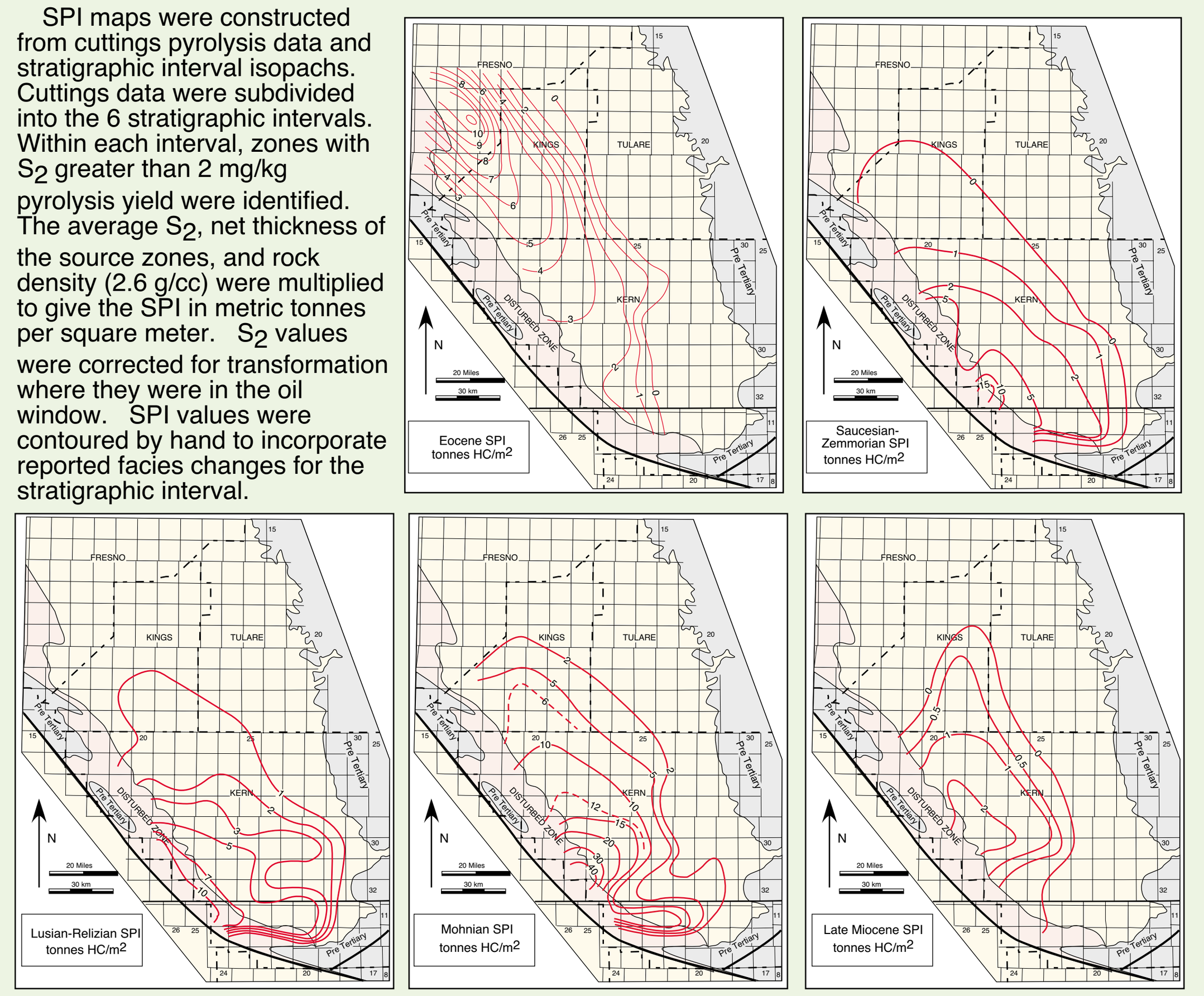

Figures: SPI maps for 5 of the 6 stratigraphic intervals. The Plio-Pleistocene interval (not shown) has no source potential. Zemmorian through Late Miocene intervals show highest SPI in the SW part of the basin. Eocene has highest SPI in the northwest. Maps have irregular contour intervals. Data are poorly constrained in the disturbed zone.

MAJOR TECTONIC FEATURES

The southern San Joaquin basin has two major depocenters (Maricopa and Buttonwillow) separated by an arch (Bakersfield - Elk Hills). The south and west basin margins are thrusted and folded due to proximity to the San Andreas fault ("disturbed zone" on map). High-relief structures extend into the basin. Most deformation is Plio-Pleistocene in age (Harding 1976). Earliest deformation is Oligocene, and most basin-center structures have grown since Miocene. The East side is relatively undeformed.

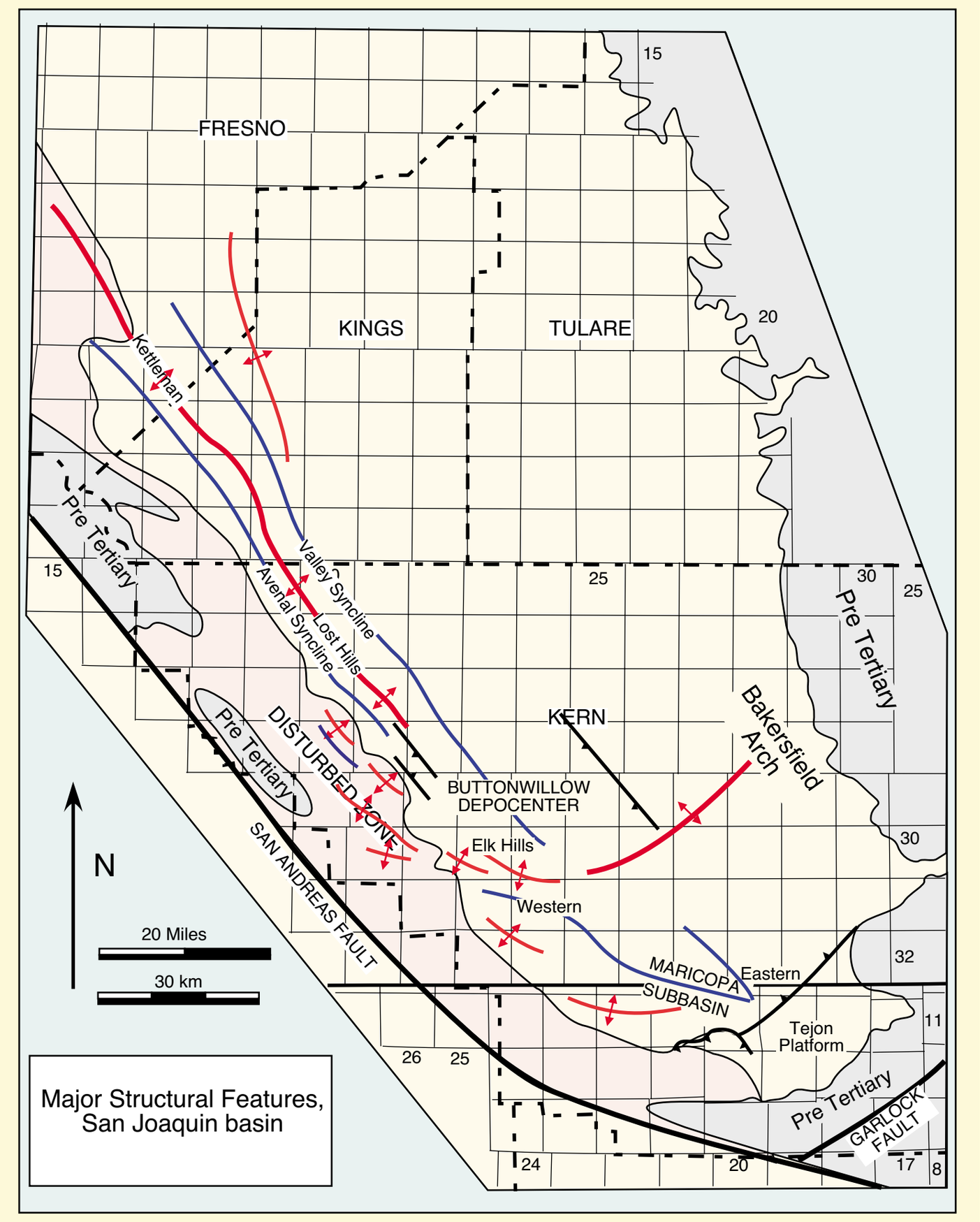

Map of major structures in the southern San Joaquin basin. Anticline axes are red; syncline axes are blue. Faults are black. Most anticlines and synclines plunge toward the two depocenters. Most structures in the western disturbed zone are not labeled.

Burial History and Transformation Kinetics

Burial and thermal history were evaluated to confirm empirical transformation relationship to temperature and to determine generation timing. Five deep wells with different thermal gradients were modeled along the basin axis. In general, there is a progressive south-to-north migration of the locus of active subsidence that results in younger generation in the north than in the south.

Transformation vs. Temperature Relationship

Kerogen transformation is a product of temperature and time, so wells with different thermal histories should show different transformation ratio at the same modern temperature. Vitrinite reflectance modeled using the Lawrence Livermore kinetics (VRLL; Burnham and Sweeney 1989) show slight differences between wells with different burial histories (see figure below). These differences are small, equivalent to less than 0.03% VRLL within the oil window. TR is fixed relative to LLVR, so this indicates that TR to temperature relationship will also be relatively constant.

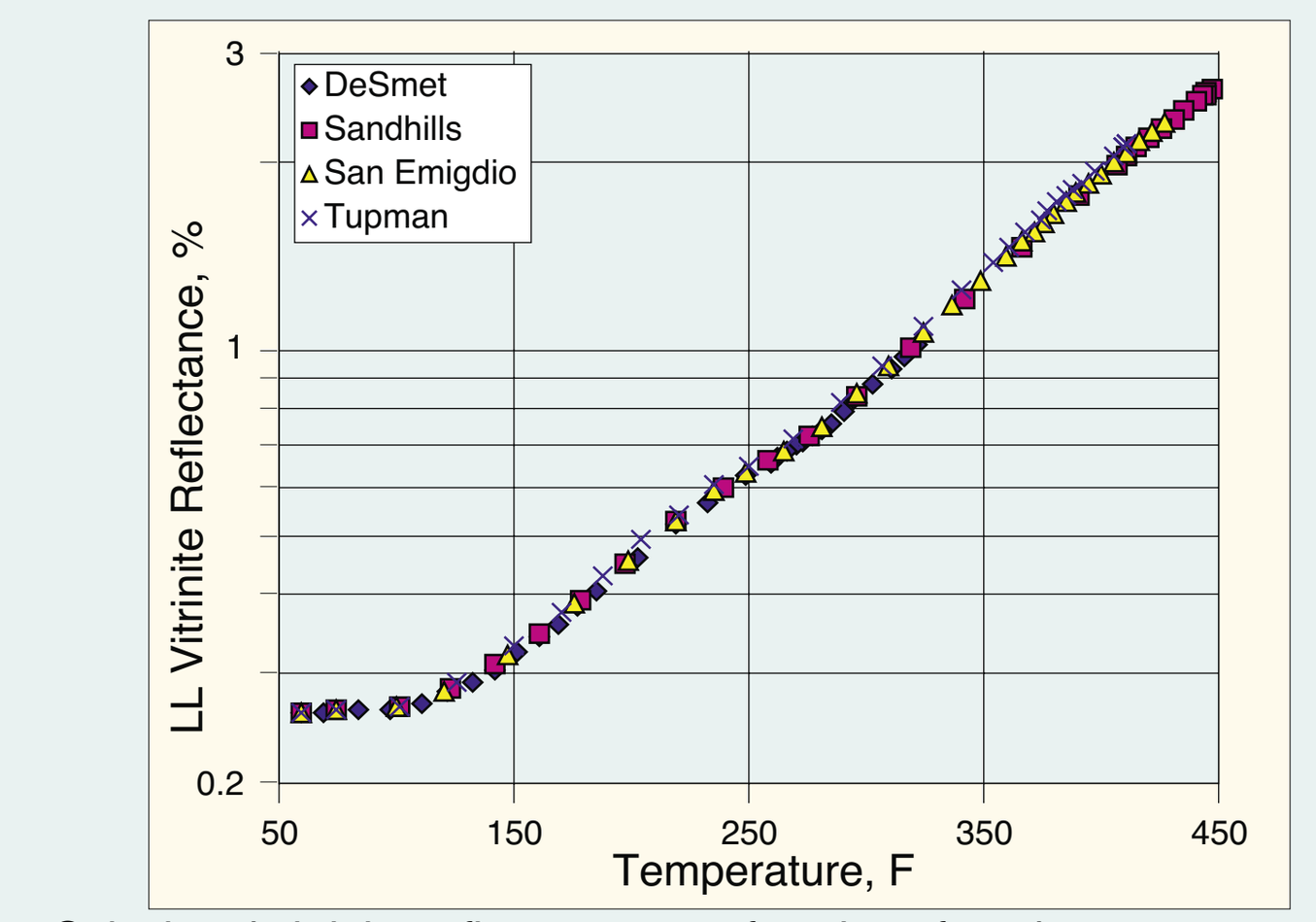

Calculated vitrinite reflectance as a function of modern temperature of 4 San Joaquin basin wells with different burial history and thermal gradient. The VR vs. T trend is essentially identical in all wells, indicating that thermal maturation can be approximated by temperature.

Kerogen Transformation Kinetics

Kerogen transformation kinetics were determined by anydrous pyrolyis for two immature Mohnian samples from Paloma field and Canfield Ranch field. These kinetics were similar to those of normal marine shales, and not similar to kinetics of sulfur-rich kerogen from the Monterey fromation in the coastal basins. Onset of generation is about 260 F and 275 F, respectively. 0.5 TR is at about 295 F and 305 F, respectively. These kinetics bracket the empirical trend at low to moderate TR (see bottom figure in section below, "Estimating Transformation). Transformation at high temperature is overestimated by kinetics.

Timing

In general, the Maricopa subbasin had the earliest generation whereas the Valley syncline had the most recent generation. Margins of both areas are actively generating today, except where uplifted by Pleistocene tectonics. Burial history curves (right) illustrate the general burial pattern, temperature evolution (color patterns), and thermal maturation (indicated by LLVR contours). Most generation is caused by Plio-Pleistocene loading.

Time of generation is indicated on the figures below. Paloma kinetics were used, because these kinetics favor early generation. Eocene horizons became thermally mature as long ago as 9 Ma in the Maricopa subbasin. Eocene generation peaks in the Buttonwillow depocenter about 5 Ma. The Valley Syncline Eocene peak generation is essentially modern.

Miocene generation initiated about 6 Ma in the central Maricopa subbasin, and peaked about 4Ma. Peak Miocene generation is about 3.5 Ma and younger in the Buttonwillow depocenter, Miocene-aged rocks have not reached peak generation in the central and northern Valley Syncline.

The great Eocene-Mid Miocene thickness under Elk Hills is inconsistent with measured vitrinite reflectance and modern temperature. The section may be tectonically thickened, or high thermal gradient may be a recent phenomenon.

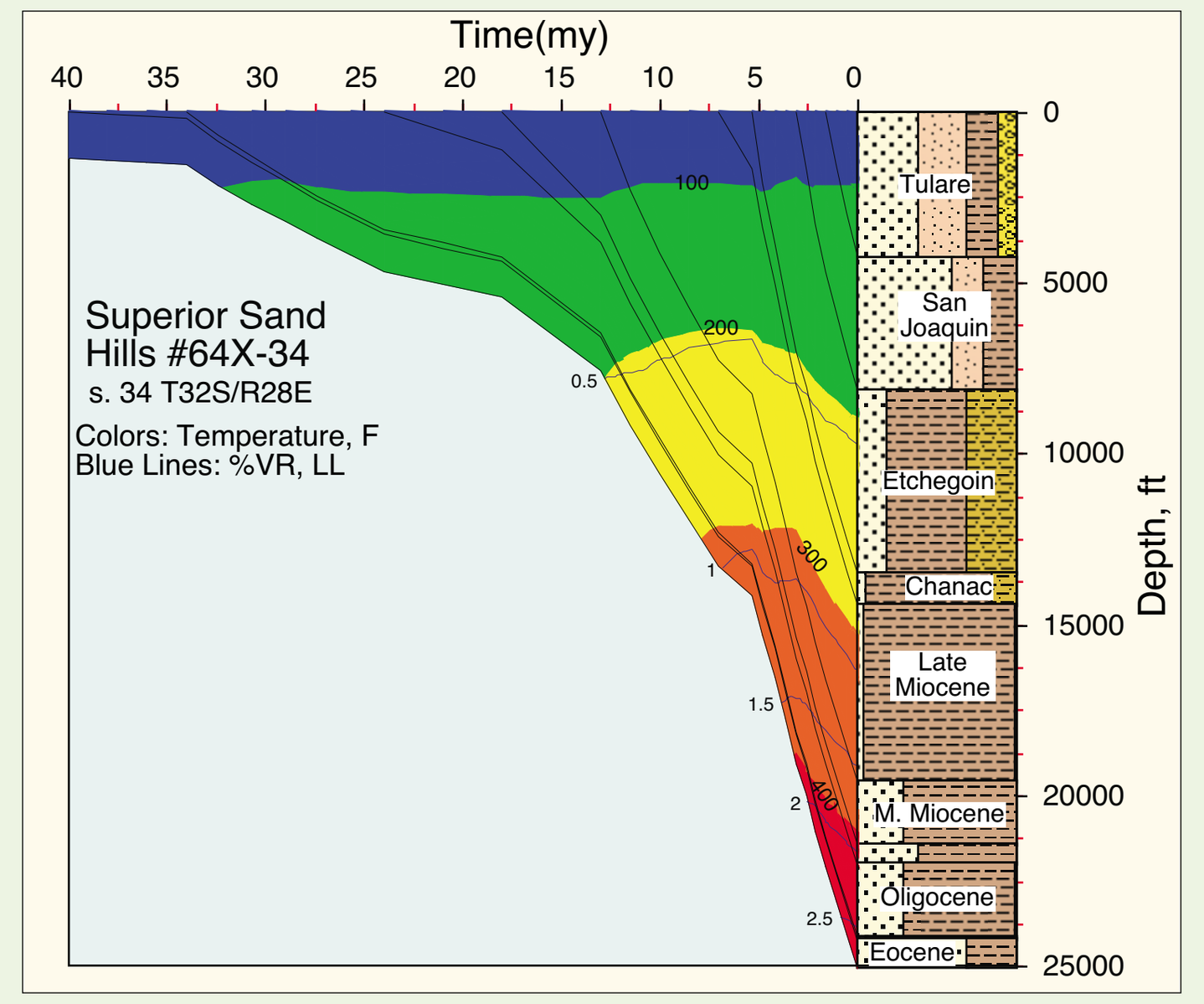

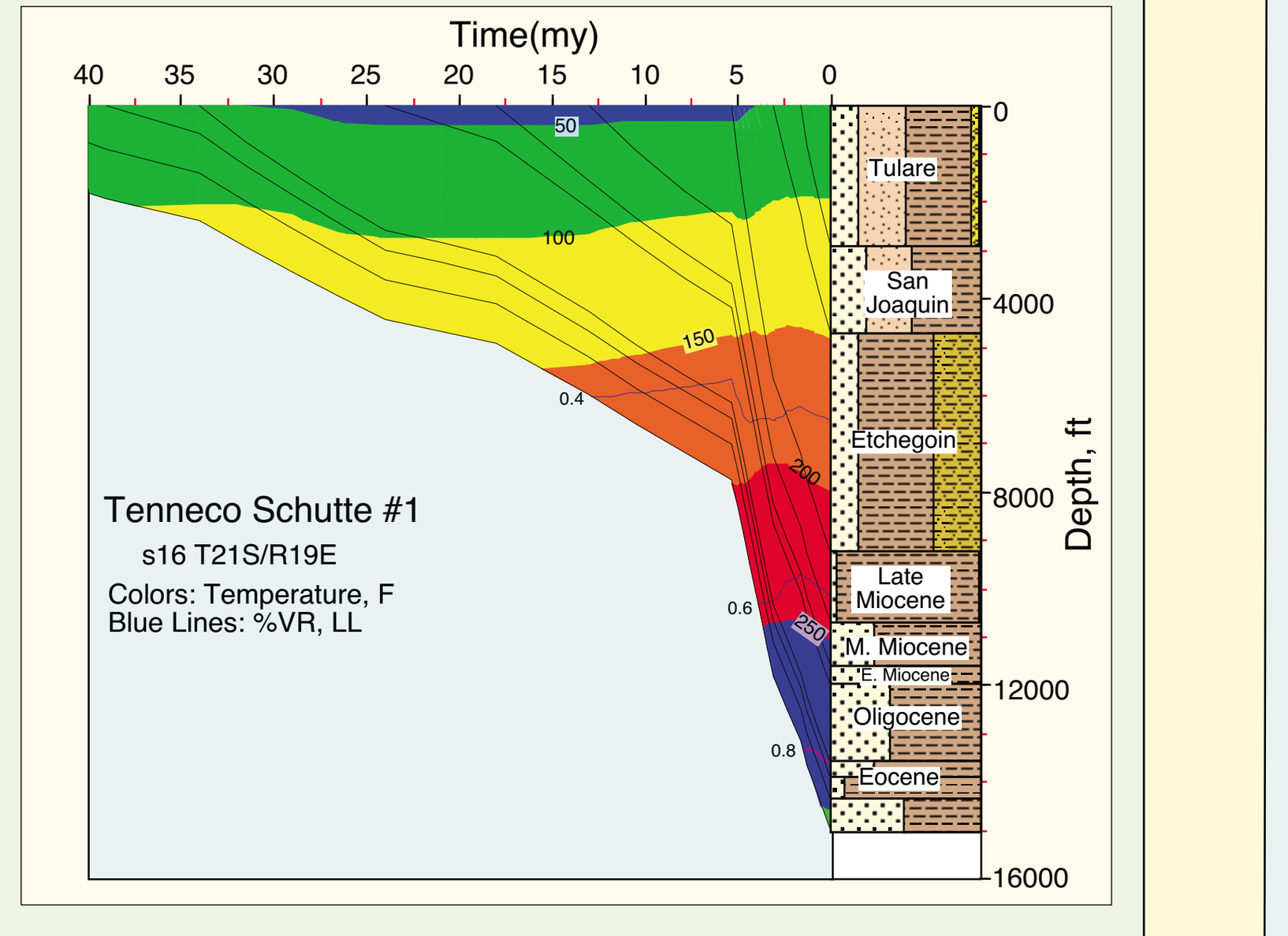

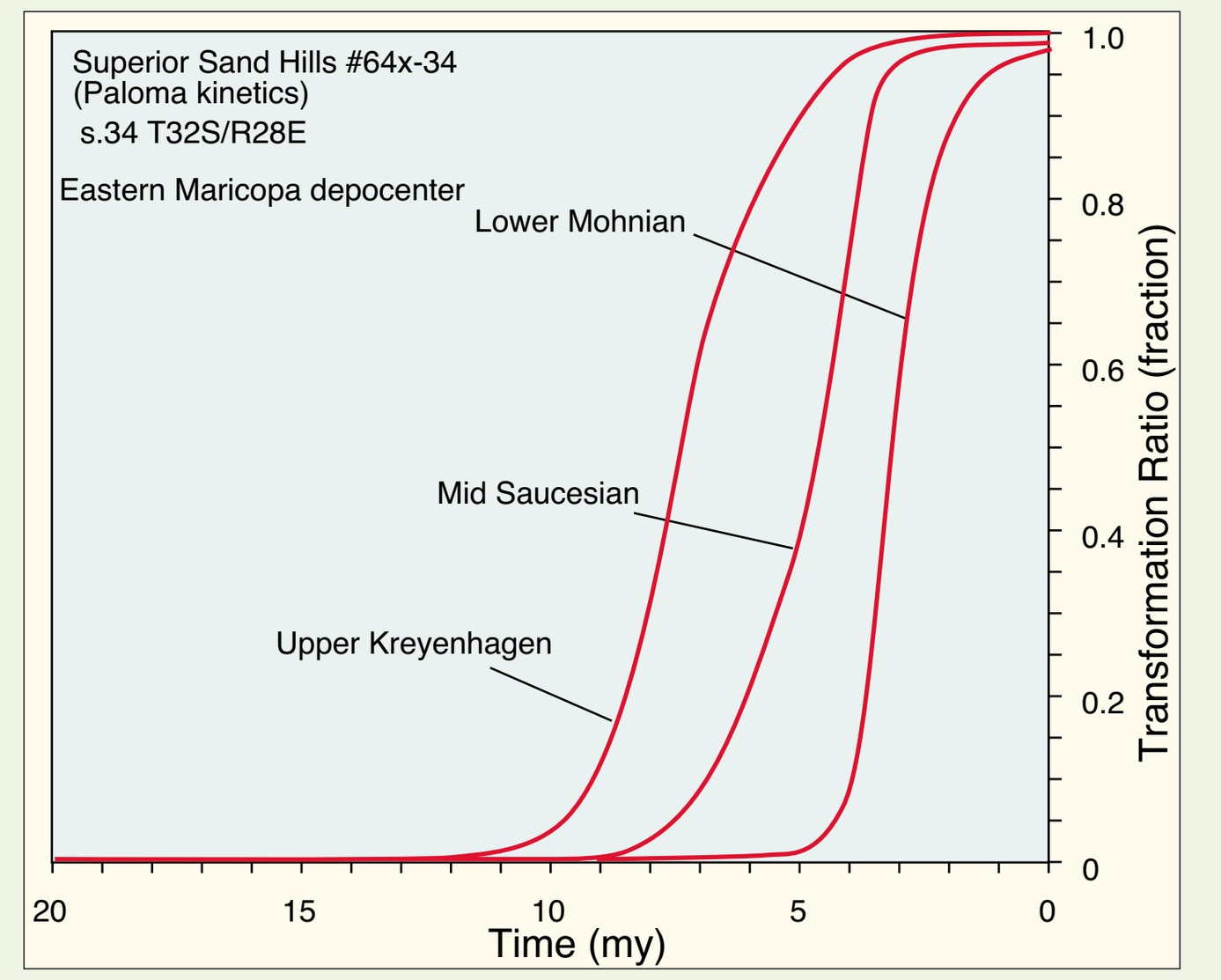

Maricopa subbasin generation history as illustrated by the Sand Hills well. Eocene horizons become thermally mature relatively early, but source quality is poor to absent here. Quality improves toward Elk Hills field, so modest generation may have occurred here prior to Pliocene deformation.

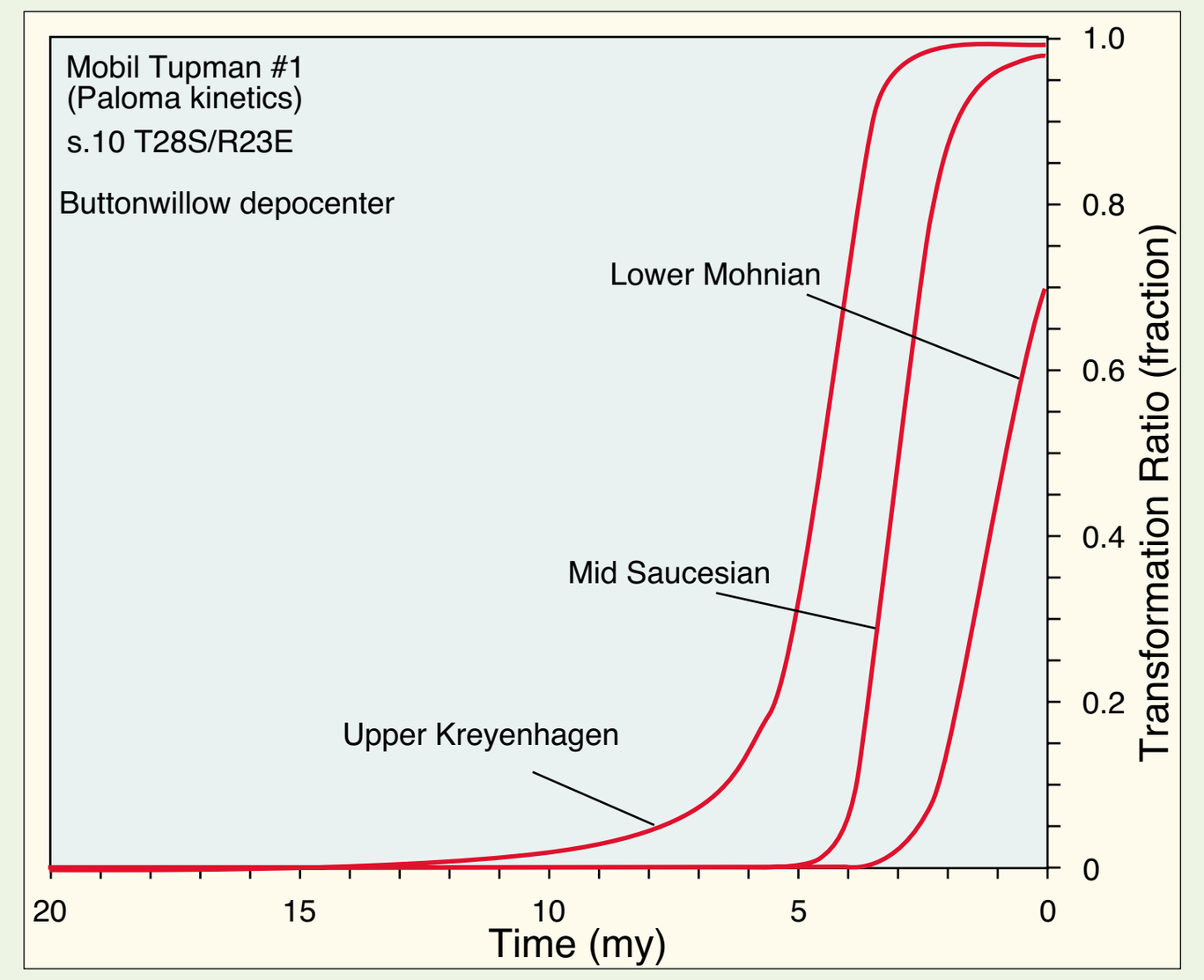

Buttonwillow oil generation as illustrated by the Tupman well. All generation is Pliocene and younger. More recent generation occurs on the eastern flank of the depocenter.

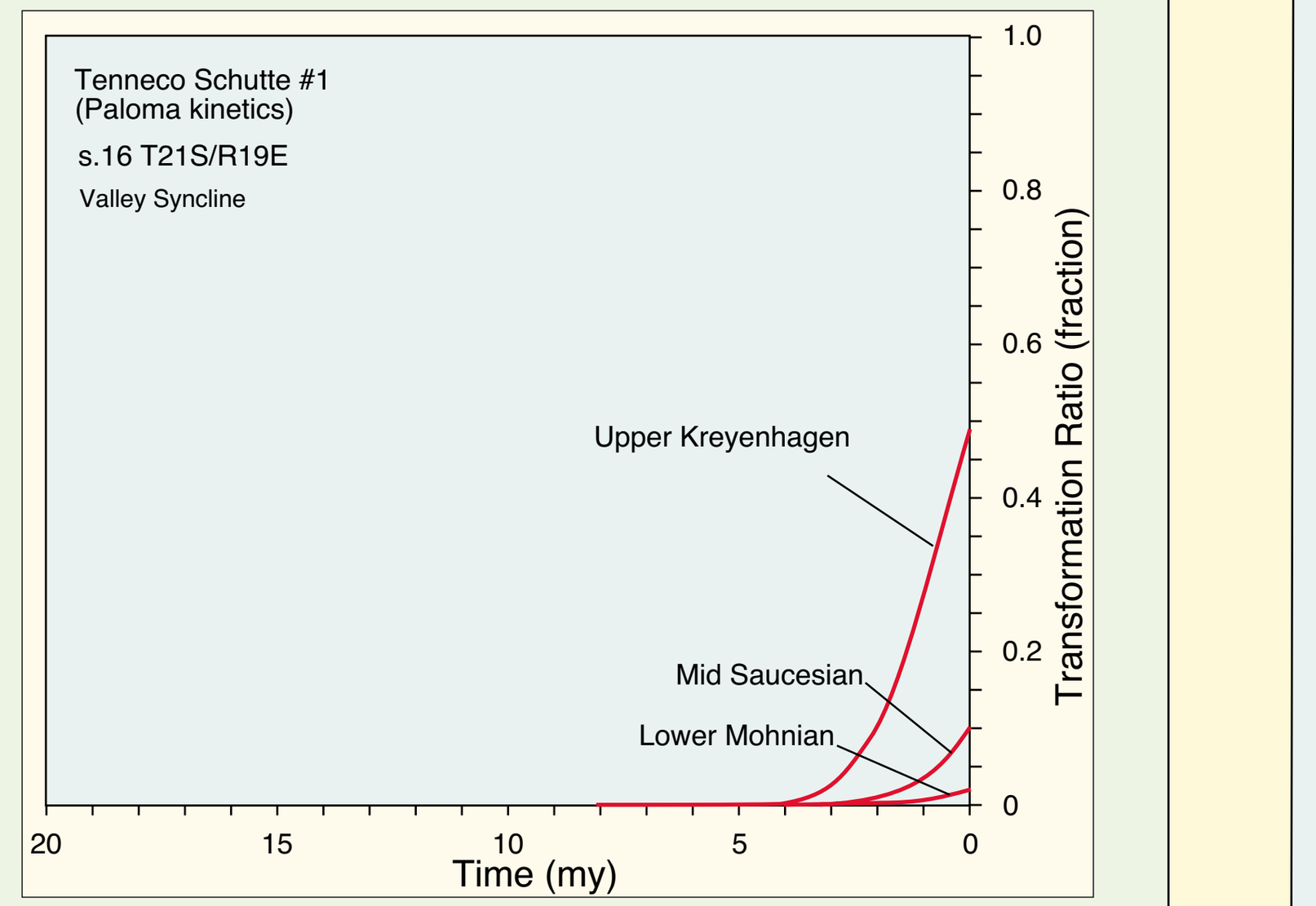

Oil generation in the central Valley Syncline as indicated by the Schutte well. The syncline plunges to the south, so age of generation becomes progressively younger toward the north. Most Miocene strata are immature or marginally mature.

Estimating Transformation

A continuous, mappable kerogen transformation function is needed for charge analysis with complex structure. Temperature, which can be calculated at all points in the basin, is used as proxy for kerogen transformation. Basin burial history curves are sufficiently similar that transformation is essentially a function of temperature in all locations where the source rocks are thermally mature. This is not strictly true, but is a reasonable approximation (see burial history, this panel).

Transformation was evaluated in two steps. First, present temperature was related to transformation ratio. Second, modern temperature distribution was converted to TR.

TR VS. TEMPERATURE

Cuttings pyrolysis S_2 (petroleum generation) for Miocene samples systematically decreases with increasing temperature. S_2 varies due to thermal maturity and source quality. The transformation component can be calculated if initial S_2 is statistically independent from present temperature, and if sufficient samples are collected to estimate either the mean, maximum or minimum S_2 at each temperature range. The transformation ratio (TR) is calculated as 1 minus the ratio of the measured S_2 (S_2^m) to the original S2 (S_2^o):

$TR = 1 - S_2^m/S_2^o$. Initial maximum or average S_2 is estimated from maximum or average S_2 at immature locations, and these are used with the observed maximum and mean S_2 data. Initiation of transformation can be confirmed by two approaches: modeling transformation kinetics and by the production index. Production index starts increasing at the same temperature maximum S_2 starts decreasing. Curves deviate due to expulsion.

Hydrogen index (HI) can also be used to estimate TR, but minor contamination of low S2 cuttings causes anomalous HI vs. temperature relationships (usually identifiable by high oxygen index). Some high S_2 outliers at high temperatures may be caused by caved cuttings or contamination.

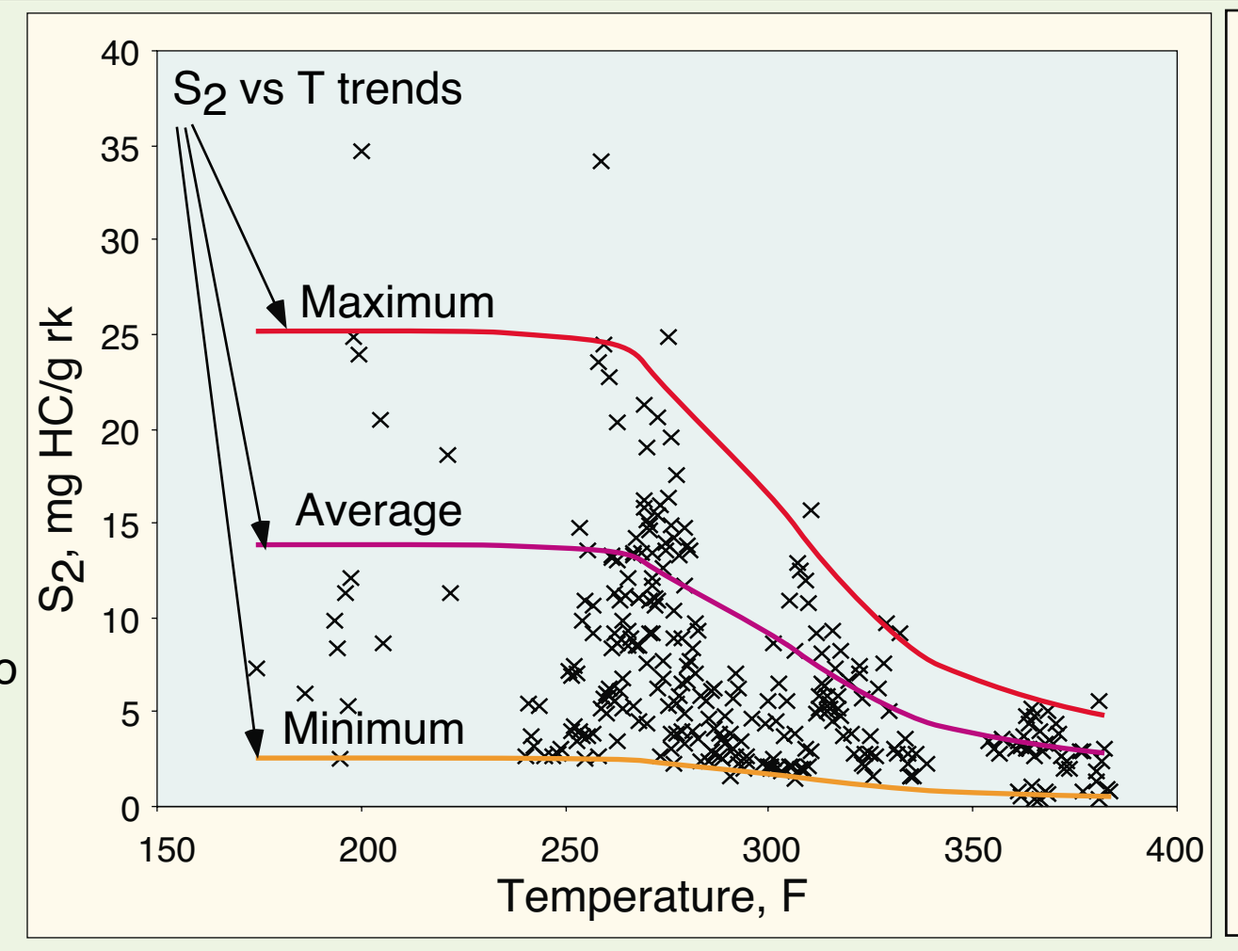

Rock eval S_2 vs. temperature for Miocene cuttings. Lines are modeled S2 vs. T trends for maximum, average, and minimum S_2. Similar trends are seen for Eocene cuttings.

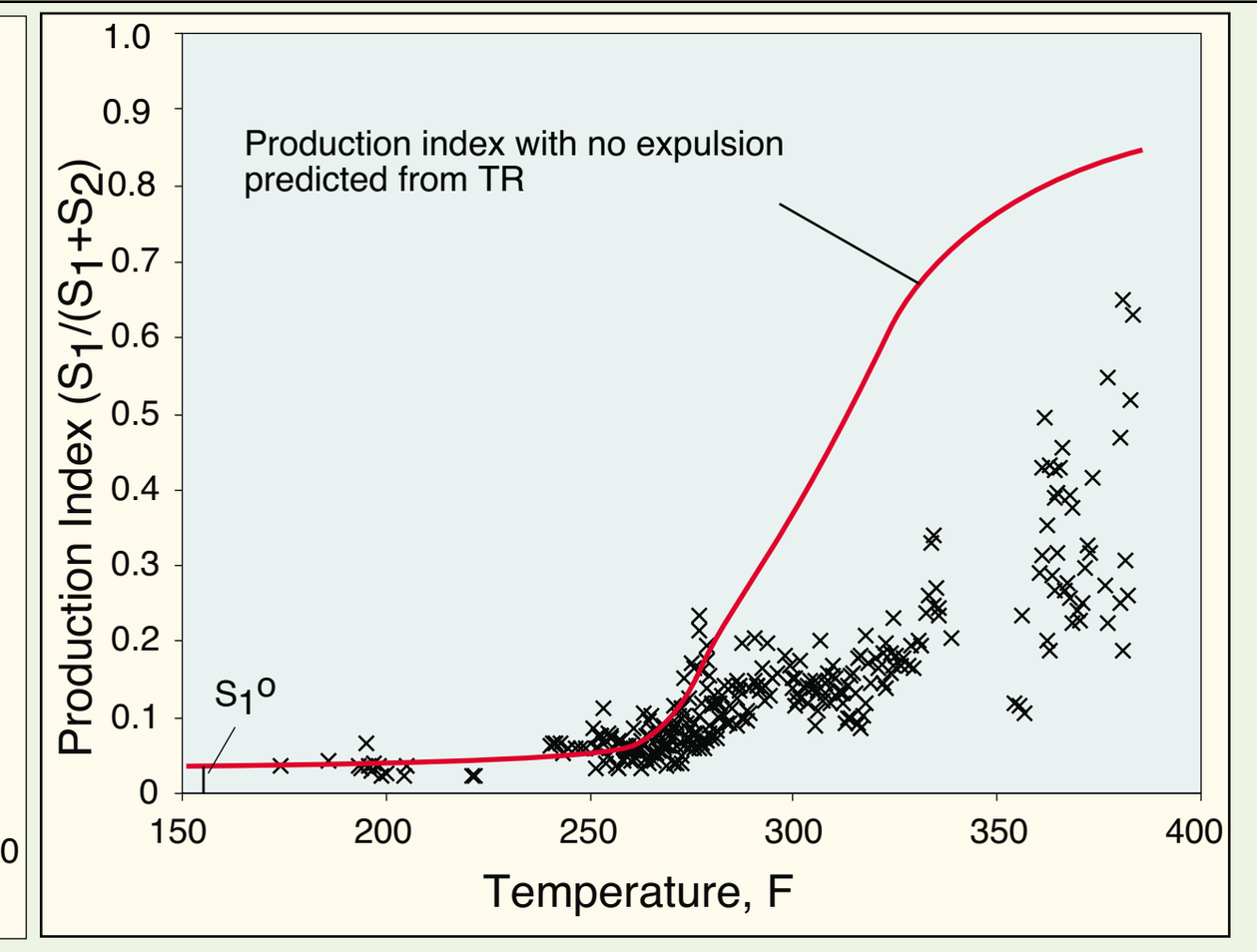

Rock eval production index vs. sample temperature. Red line is predicted production index with no expulsion.

Comparison of empirical TR vs T trend with kinetics calculated from anhydrous pyrolysis. Empirical data show similar TR at low and moderate temperatures, but lower TR at high thermal maturity. The empirical trend is consistent with observed deep oil shows, so it is believed closer to correct. The empirical trend was used for calculating petroleum generation from all source rocks using modern temperatures.

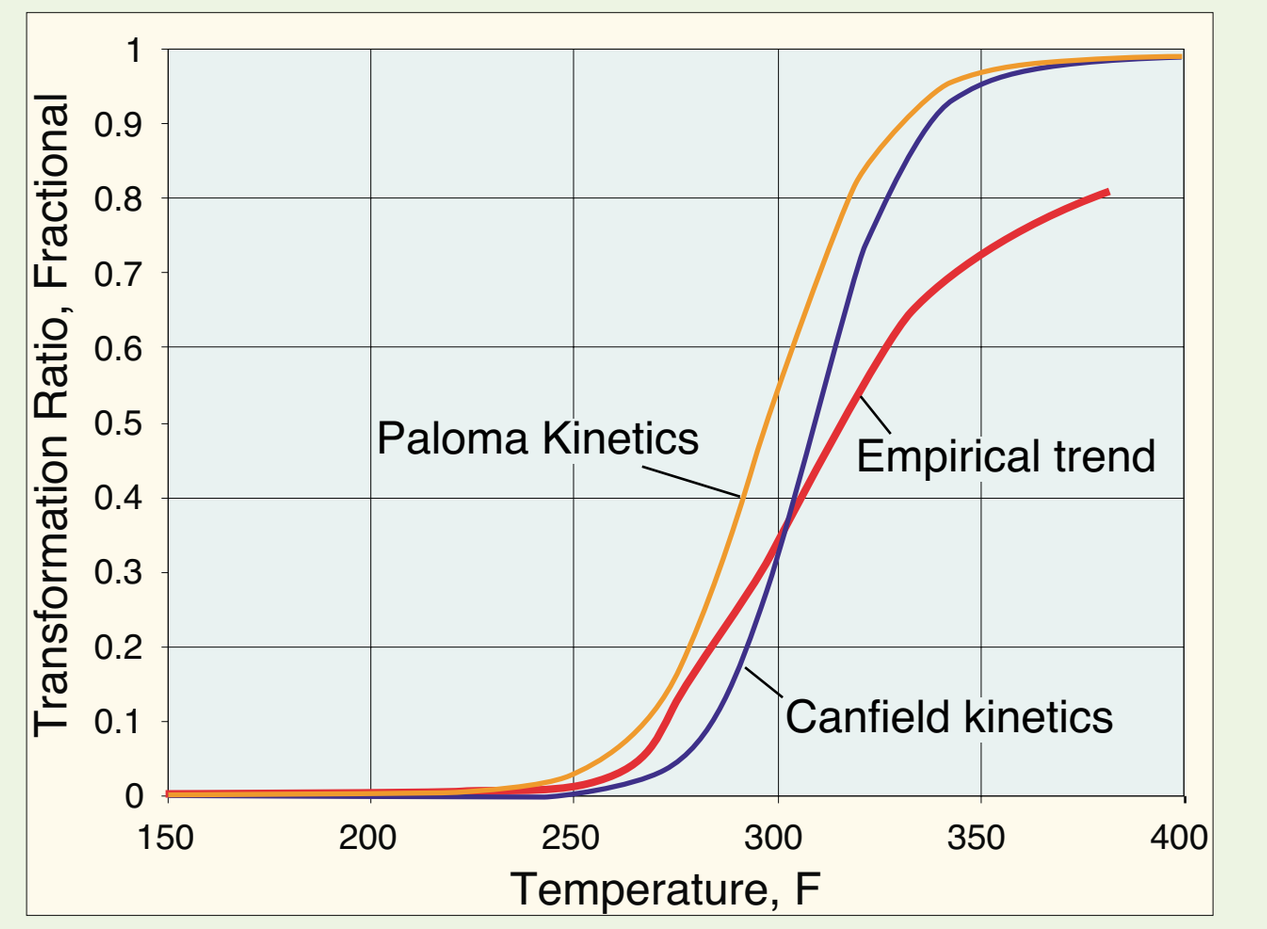

TEMPERATURE DISTRIBUTION

Subsurface temperatures were estimated from bottomhole temperatures (BHT). Temperatures were corrected with an empirical function calibrated to local equilibrated well temperature data. Individual BHT data have low reliability that introduces scatter to thermal gradient maps. Data from nearby wells (within 5 km) were plotted together to form a more statistically reliable temperature vs. depth trend.

Both equilibrated wells and corrected BHT data show decreasing thermal gradient with depth. This effect is incorporated into the thermal gradient map by a polynomial function. Temperature (T) at a subsurface depth in feet (D) is calculated from the mapped thermal gradient (TG) using the following formulas:

$$T = (TG - 0.00005(D - 10000))D/100 + 60; \; D \leq 10,000;$$
$$T = (TG - 0.5)/100(D-10000) + 100(TG) + 60; \quad D \geq 10,000$$

Modeled heat flows range from about 50 to 58 mW/m^2, consistent with published SJB heat flow.

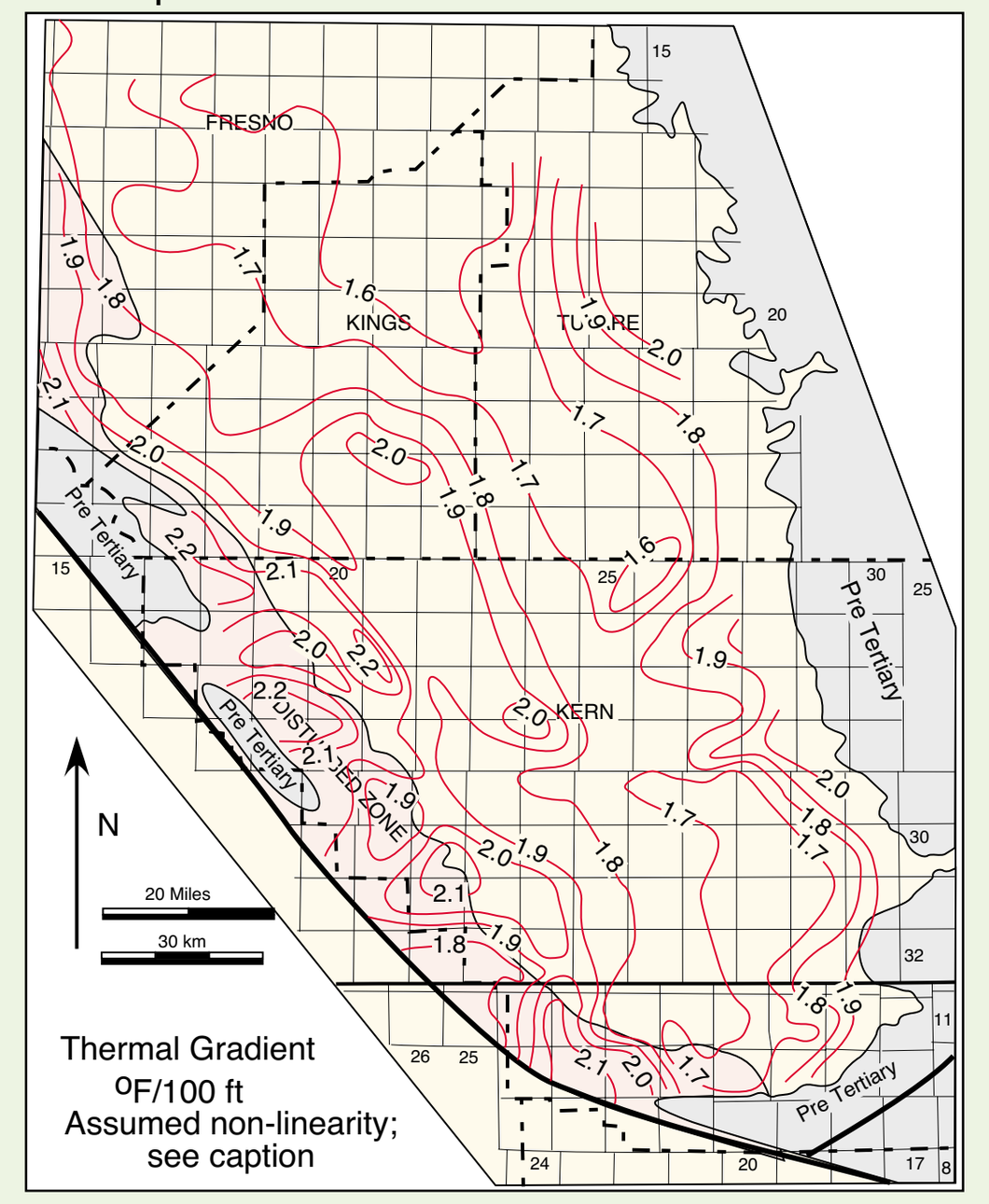

TRANSFORMATION MAPS

Temperature at the top and base of each stratigraphic unit was calculated from the non-linear thermal gradient and subsurface depth. Temperatures wered converted to TR. The TR at the top and base of each unit was averaged at each point and mapped (see example below). Contour units are the fraction of the total SPI which has been converted into petroleum.

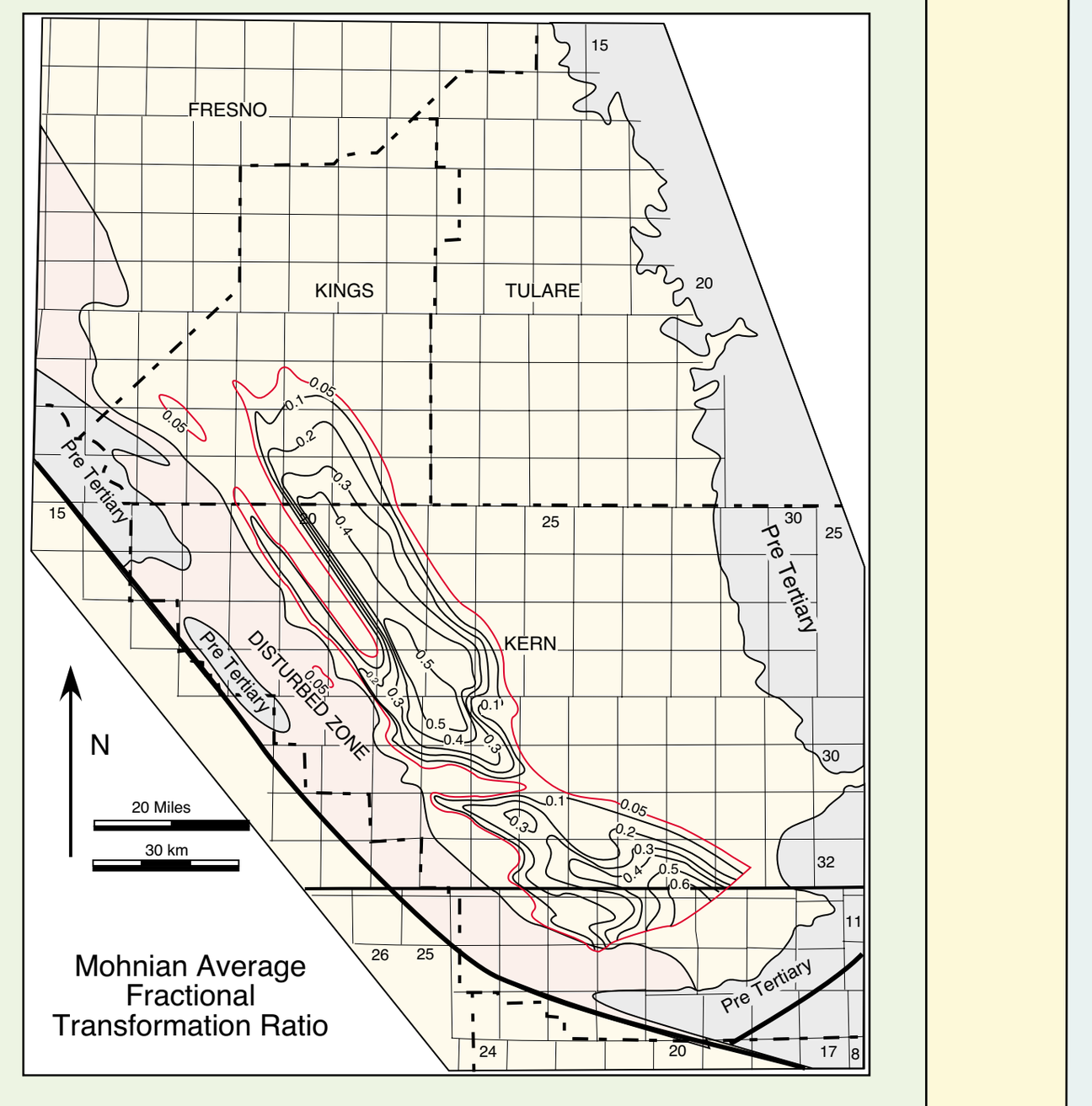

Example transformation ratio (TR) map of the Mohnian interval. TR of 0.05 (red) is minimum plotted TR because this is the minimum TR associated with expulsion (see next panel).

CHARGE ANALYSIS RESULTS

PETROLEUM GENERATION

Petroleum generation per unit area was estimated by multiplying the SPI by the TR. Total generation is calculated from the generation maps. The total generation is about 200 billion BOE, compared to an in-place oil of about 50 billion BOE, so overall basin trapping efficiency is about 25%.

The Mohnian section has the highest SPI, but its total generation is only slightly greater than that of The Eocene and Lower Miocene - Oligocene interval due to lower average TR. Generation by area and stratigraphic interval is summarized in the following table.

Eocene and Zemorrian-Saucesian generation is not mapped far into the western Disturbed zone due to lack of high quality transformation and SPI data. General generation patterns and timing are discussed on the third panel. Middle and Late Miocene source rocks are immature in the disturbed zone except where mapped below.

Petroleum Generation, million BOE

Unit	Location						
	Avenal Syncline	Valley Syn. (Kings and Fresno Cos.)	Valley Syn. (Kern Co., 727 and N)	Buttonwillow Depocenter	Western Maricopa Subbsn.	Eastern Maricopa Subbsn.	Total
Plio-Pleistocene	0	0	0	0	0	0	0
Late Miocene	1	75	485	773	6	0	1340
Mohnian	1211	5476	14,731	22,081	5242	9776	58,516
Luisian - Relizian	423	1313	4131	9959	8455	12,763	37,044
Zemmorian - Saucesian	190	1782	5412	12,359	17,504	11,182	50,150
Eocene	6439	17,637	14,097	10,521	5540	611	54,845
Total	9981	26,283	38,859	55,693	36,748	34,332	201,895

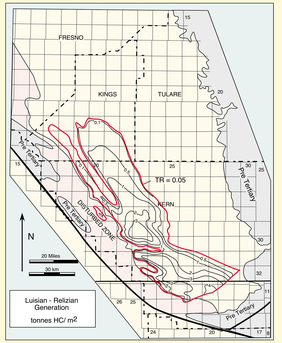

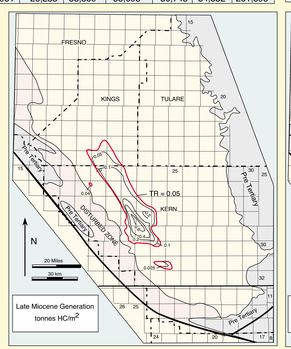

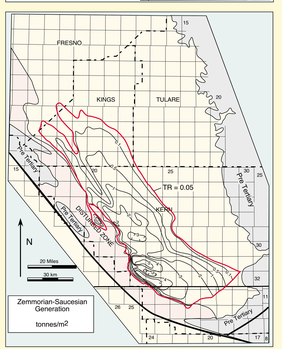

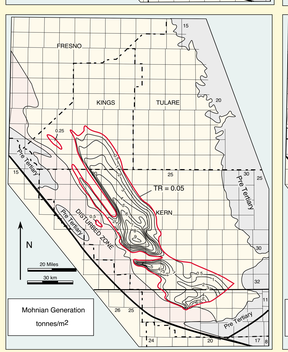

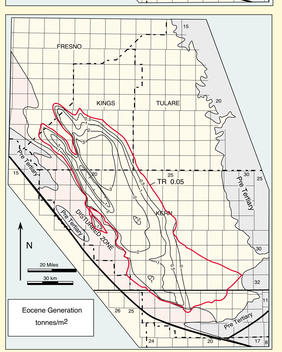

EXPULSION EFFICIENCY

Expulsion efficiency (EE) is the fraction of the generated petroleum which has left the sample (Pepper 1991):

$$EE = \frac{\text{expelled HC}}{\text{generated HC}^{-}} = \frac{\text{generated HC + initial HC - retained HC}}{\text{generated HC + initial HC}}$$

EE can be calculated from TR, pyrolysis S_1, and pyrolysis S_2. S_1 measures HC retained in the sample, which can be corrected for volatile loss from GOR and oil distillation curves (S_1-c) of petroleum generated from the source rock at a given transformation level. The generated petroleum is the initial S_2 (S_2^o) multiplied by the TR. S_2^o is the measured S_2 (S_2^m) divided by (1 - TR). EE can therefore be approximated from the following relationship:

$$EE = \frac{S_2^m \frac{TR}{1\text{-}TR} + S_1\text{-}0 - S_1\text{-}c}{S_2^m \frac{TR}{1\text{-}TR} + S_1\text{-}0}$$

Expulsion efficiency was calculated from the same Miocene cuttings data used to estimate transformation. The S_1 correction factor (S_1-c^o/S_1) varies from 1 at TR = 0 to 1.17 at TR = 0.5 to 1.4 at TR = 0.8.

Expulsion efficiency is a function of TR and source richness. At low TR, individual samples show both negative and positive EE because of variable S_1-^{o} and because EE is calculated by subtracting one small number from another, which sometimes gives negative results. The average EE is zero from TR = 0 to TR = 0.05. At higher TR, average EE is positive, and no negative EE are measured beyond TR = 0.15. The average EE trend rapidly rises to values exceeding 0.7 by TR = 0.3 and approaches 0.9 at TR = 0.8 (see figure below). Much of the scatter at high TR is related to variable source richness. Much of the scatter at low TR is probably caused by poor estimates of TR. EE variation with richness will not be discussed.

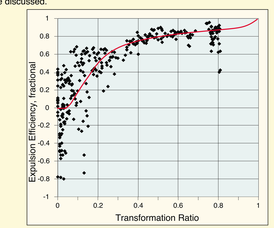

Results are similar to a simple saturation expulsion model, such as that proposed by Pepper (1991). A saturation of about 0.1 times the S_2^o is characteristic of most of the oil window.

For an S_2^o original of about 15 mg HC/g rk, petroleum saturation during expulsion is about 1.5 mg/g rk. Unlike Pepper's model, some expulsion begins before complete kerogen saturation. This is expected from percolation theory because the percolation threshold is less than complete saturation. High expulsion at high TR is modeled on the assumption that complete transformation (graphitization) causes complete expulsion.

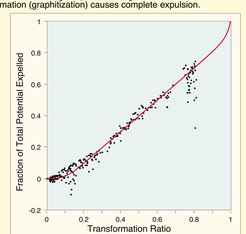

IMPLICATIONS

High expulsion efficiency means that most generated petroleum is expelled and that small EE variations do not cause major fractional expelled petroleum variation. A relatively constant EE value of about 0.7 to 0.8 can be used over most of the range of TR. Marginally mature units (such as the Late Miocene and Mohnian layers) may have significant petroleum generation, but less expulsion than layers with similar petroleum generation at higher transformation.

SECONDARY MIGRATION PATTERNS AND EFFICIENCY

INTRODUCTION

Migration efficiency was estimated by comparing the amount of petroleum within an accumulation to the petroleum generated in a position that can charge the accumulation. The petroleum in place is taken from published and unpublished sources. Charge is estimated by determining the fetch (drainage) area for an accumulation and integrating the petroleum generation within the fetch area. In the San Joaquin basin, secondary migration is mainly controlled by structural dip, with a secondary control by stratigraphic heterogeneities. Along-fault migration is relatively modest due to the sparsity of large-throw faults in the areas and depths of petroleum generation.

DEFINING FETCH AREAS

The steep dips, high degree of stratification, and good seals constrains most migration to follow an updip migration pattern along carrier beds. Most generation is Quaternary, so modern structure along the tops of each stratigraphic interval are used to define the migration direction. Structural drainage to traps or areas within the San Joaquin basin are defined by structural divergences within the various petroleum systems. Fetch area therefore varies with stratigraphic position. Major updip pinchouts of carrier beds cause stratigraphic focusing oblique to the updip direction. This affects migration in parts of the disturbed zone and the Edison-Mountain View field area.

Faults influence migration in two ways: along-vault vertical migration up transmissive faults and oblique migration against sealing faults. Oil probably migrates up faults in the vicinity of Cal Canal field and along the White Wolf fault. Drainage areafor fault migration is still controlled by dip patterns in surrounding rocks. Deflection of migration from regional dip by sealing faults occurs mainly along the Wasco-Rio Bravo fault zone and along small-displacement faults on the eastern side of the basin. Offset of these small-displacement faults is insufficient to affect regional migration patterns, but the Wasco-Rio Bravo and Jerry Slough-Bowerbank faults focus petroleum toward the Bakersfield arch.

Little or no generation occurs in the western disturbed zone, so major faults in this area only affects the updip part of the migration pathway and trapping configuration. Migration patterns in this complex area are not investigated in detail.

Regional seals thin towards the updip parts of the petroleum systems, so oil generated in the different stratigraphic intervals mix and charge shallower reservoirs. Charge to different pools on the structure were not differentiated because of the potential for mixing. Immature upper Miocene sealing strata at the north end of the basin favors downward expulsion of petroleum generated from lower and Middle Miocene rocks. This oil mixes with Eocene-generated oil in the Temblor system.

TIMING ISSUES

Although charging is recent, structural deformation has continued to today. In most areas, structural growth has continued in about the same areas since inception of generation in the Late Miocene. the eastern margin has continued to be exhumed as the basin center sinks. this enhances dip magnitude but does not significantly alter dip direction. Fetch areas drawn with present day structure are not significantly altered by differential structural growth.

This assumption is not valid in all areas. In the Coalinga area and other parts of the disturbed zone, there is evidence for structural inversion. For example, the Vallicitos area (immediately north of the study area) is now a synform. It was an anticline prior to Inversion after San Joaquin Formation deposition and before/during Tulare Formation deposition. In another example, thrust faulting east of McKittrick field has altered charge patterns to Belgian Anticline.

Timing is less likely to be an issue for east-draining areas and traps charged by younger (Miocene) source rocks. Eocene oil generation began earlier, so its distribution is more likely affected by structural alteration of migration patterns.

MIGRATION IN CHAIN AND NET PATTERNS

The San Joaquin basin is characterized by high charge volume, so most traps fill and spill to other traps. The migration efficiency calculated for a spilling or leaking trap does not accurately reflect migration losses, because unaccounted petroleum may have been spilled from the trap, not lost on the way to the trap. To minimize this effect, petroleum accumulations are divided into three categories: simple charge, migration chains, and migration nets. Simple charge is charge to a petroleum accumulation without passing through other known economic accumulations first. A migration chain develops where economic accumulations spill into other, shallower accumulations to form a chain of accumulations along the migration pathway. A migration net forms where one accumulation may spill or leak to two or more accumulations simultaneously, or where there are two potential spillpoints at approximately the same elevation. This occurs in traps with a stratigraphic component or a weak seal and a high charge rate.

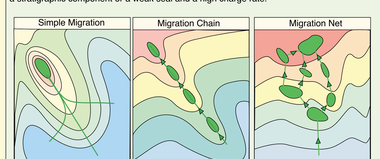

RESULTS

Estimated oil-in-place and charge to different structures and areas are summarized in this table. Limits of drainage areas are not mapped because the boundaries change with stratigraphic interval. Numbers referring to fields in the fetch areas are shown on the maps below. Large numbers of fields are grouped because spillage is common in the basin, and most fields are parts of migration chains or nets. Northern Eocene-charged fetch areas include a small amount of admixed Miocene-generated oil where Miocene strata are thermally mature.

One metric tonne of 30^o oil equals about 7.5 barrels.

Fields	Area #	Oil type	OPIP, MM t	Charge, MM t	Gathering Area, km²	Drainage Area, km²	Migration distance, km	Migraton Efficiency, %	Comments
Helm, Raisin City, Burrel, Riverdale, Camden, San Joaquin	1	E	67.0	845.4	405	1332	60	8	
Cantua Crk, Cantua Nuevo, Turk Anticline	2	E	0.3	10.2	18	379	40	3	Drainage area probably overestimated
Coalinga + Kettleman domes + Guijarral Hills + Pleasant Valley	3	E	1380.1	1340.0	915	1436	60	103	Possible Cretaceous charge in north; Seepage, Tar seals; Only Eocene charge from Lost hills area
Jacalitos	4	E	12.7	16.0	25	190	22	80	Probable Cretaceous charge; Possible spill to Coalinga
Kreyenhagen	4.1	E	0.012	0.2	1.4	7	5	5	Tar seal on small accumulation
Pyramid Hills	5.1	E	5.5	10.5	13	70	6	52	Biodegradation, tar seal (part)
Devil's Den	5.2	E	2.6	20.7	16	72	6	13	Biodegradation, Tar seal (part)
Welcome Valley	5.3	M	0.016	12.2	6	25	9	0.13	Tar seal on small accumulation
Blackwells Corner + Beer Nose	5.4	E	4.5	61.5	34	82	9		Tar seal on small accumulation
Lost Hills +Belridge	6	M	711.0	1547.1	503	735	12	46	Tar seals, biodegradation
Belridge	6	E	99.3	179.5	153	236	8	55	
Antelope Hills, N	7.1	E	5.4	9.3	10	43	5	54	Assumes focused migration from N. on Aqua truncation
McDonald A. + Antelope Hills	7.2	E	15.6	35.1	21	62	8	44	Local tar mat
Cymric	7.3	M	139.0	175.8	34	137	15	79	Biodegradation, Tar seals
Cymric	7.3	E	40.0	72.1	65	110	13	56	
Chico-Martinez	7.4	M	0.32	1.3	3.8	17	2.5	24	Only charge from Middle Monterey; tar seal
Railroad gap + McKittrick	8	E	48.1	65.4	60	73	9	74	
Buena Vista	9	M	468.0	1324.5	214	268	8	35	Minimum ME est.; possible spillage into Midway-Sunset
Belgian A. + Asphalto +Buena Vista	9	E	66.7	180.2	278	406	40	37	Assumes migration before McKittrick Fault
Midway-Sunset + Asphalto + McKittrick SE + Yolumne + San Emidio Nose + Landslide + los Lobos	10	M	1045.8	2320.7	382	636	45	45	Seepage, biodegradation at M-S.
Midway Sunset	10	E	0	137.6	254	295	15	0.00	Insufficient deep tests
Elk Hills + Railroad Gap + McKittrick	11	M	829.0	2062.2	285	347	19	40	Seepage
Elk Hills + Coles Levee	11	E	0	271.5	402	402	9	0.00	No permeable reservoir at depth
Bakersfield Arch (all) + Coles Levee, N &S + Paloma	12	M	1677.0	4580.1	2239	4031	45	37	Assumes all NCL spill to east
Kern Bluff	13.1	M	11.7	29.1	22	119	31	40	
Art Hill + Edison + Mountain View	13.2	M	291.0	424.1	173	468	25	69	
San Emidio Creek + Eagles Nest	14.1	M	0.03	15.2	1.4	11	3	0.20	Poorly defined drainage area
Whitewolf	14.2	M	1.4	28.5	8.6	17	1.25	5	Poorly defined drainage area
Pleito	14.3	M	11.0	31.3	5.7	12	1.5	35	
Comanche Point	14.4	M	0.09	8.7	4.8	26	10	1	Poorly defined drainage area
Wheeler Ridge	15.1	M	43.0	61.7	10	27	4	70	
Tejon +Tejon N.	15.2	M	46.0	92.4	19	932	12	50	
Tejon Hills	15.3	M	5.5	16.0	6.7	100	13	34	
Eastern Area, N. of Wasco-R. Bravo Trend	16	E + M	2.5	1978.6	965	5018	50	0.13	Few traps discovered

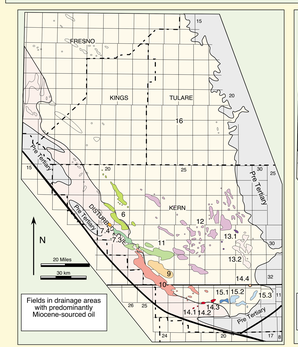

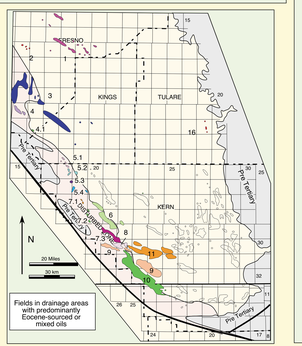

DISCUSSION AND INTERPRETATION

MIGRATION EFFICIENCY CONTROLS

Migration efficiency of large fetch areas charged primarily by Miocene oils show reasonably consistent migration efficiency near 50% where migration distance is 30 km or less. Migration efficiency decreases with migration distance to about 10% at 60 km. Lack of systematic decrease for short migration distance may be caused by migration through thermally mature rock, where losses are expected to be less. Scatter is probably related to both variable carrier bed lithology and errors in oil-in-place and charge estimates. Decreasing efficiency with longer migration distance is probably related to losses associated with charging the migration pathway and maintaining a partial oil saturation outside of known field boundaries.

ANOMALOUS COALINGA - NORTH KETTLEMAN MIGRATION EFFICIENCY

The fetch area including Coalinga and North Kettleman fields has a migration efficiency exceeding 100 %, which is theoretically impossible. Possible reasons for this are the following: underestimated TR, underestimated SPI, underestimated expulsion efficiency, admixed Cretaceous sourced oil, or changes in drainage areas. TR and SPI are reasonably consistent, and change to 100 % expulsion efficiency will not lower migration efficiency to near 80 %. Admixed Cretaceous-sourced oil would probably be detected if over 20% of the oil volume, which is still insufficient to lower efficiency to levels seen in other fetch areas.

The most likely cause for the high apparent migration efficiency is a change in fetch area configuration. The Coalinga nose is an old feature, which apparently extended south along the Kettleman-Lost Hills axis since Oligocene deformation. Late Miocene generation of Eocene oil in the Buttonwillow depocenter and southern parts of the Valley Syncline that are not in the present structural fetch would drain towards the north prior to Plio-Pleistocene deformation. This would take oil from areas 1, 5, and 6 and divert it to areas 3 and 4. Oil migrating through the Coalinga area would charge the Vallicitos area prior to its Pleistocene inversion.

EFFECT OF FETCH SIZE ON MIGRATION EFFICIENCY ESTIMATION

The small drainage areas show the most scatter, and generally the lowest migration efficiency. High scatter is caused by the use of regional structure to define fetch areas. Small amounts of stratigraphic focusing, minor faulting or minor faulting undetectable on a regional scale can greatly affect local migration patterns. Mapping was based on regional patterns, and individual fetch areas were not mapped with high resolution due to unavailable data.

The generally lower migration efficiency of smaller accumulations is probably related to three factors. First, seepage and biodegradation associated with tar seals affects a greater fraction of the charge to small fields than to large fields. Second, small drainage areas with small fields are identified specifically because they had lower charge that prevented the formation of migration chains or nets. This situation is most likely to develop where charge is relatively small. Third, fetch areas were probably systematically overestimated for small fields, especially along the west side of the basin, because migration patterns are parallel and unfocused, but the drainage areas were systematically divided between fields. Migrating oil which "missed" the fields due to their small focus were inadvertently included in one drainage or another.

SECONDARY MIGRATION EFFICIENCY

Known petroleum trapped in a fetch area can be compared to the petroleum expelled from source rocks in the fetch area to estimate secondary migration efficiency. The top figure is a plot for all drainage areas assessed. Most drainage areas with high charge form a trend of increasing known petroleum in place with increasing charge. Drainage areas with low charge show significant scatter. Scatter is related to three factors: seepage losses, undiscovered accumulations, and poorly defined fetch areas. Data for fetch areas with significant macroseepage are circled. Data for poorly defined fetch areas are outlined with green squares. Seepage does not affect large accumulations because seepage losses are small compared to reservoired petroleum.

Migration efficiency may also reflect potential undiscovered petroleum. The large drainage areas associated with major fields and trends are unlikely to be significantly affected by future discoveries, but small drainage areas may be. Note that the one large charge area with low migration efficiency is the northeast side of the basin. It is unclear whether this is related to undiscovered accumulations or low migration efficiency due to absence of traps. Most drainage areas charged by Eocene petroleum in the southern part of the basin have no discovered petroleum, so their calculated migration efficiency is zero. This is partially related to absence/deficit of deep drilling.

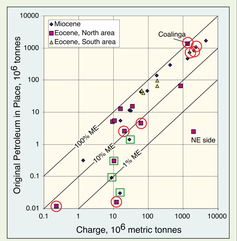

Comparison of charge (petroleum expelled from source rocks) to original petroleum in place (oil + gas, excluding bacterial gas, but including the biodegraded parts of oil and asphalt). Data for drainage areas with known significant macroseepage are circled. Data for drainage areas with poorly defined boundaries are outlined by green squares. Some fetch areas with no economic petroleum reserves are not plotted on this logarithmic plot.

One metric tonne of 30^o oil equals about 7.5 barrels.

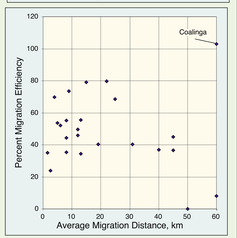

Migration efficiency as a function of average migration distance for large fetch areas. For short migration distances (less than 30 km), about half of the expelled oil is trapped in discovered economic accumulations. Past an average migraiton distance of 30 km, migration efficiency decreases. Scatter may be related to variable nature of migration pathway, variable potential for future discovery, or systematic differences in migration efficiency. The drainage area including Coalinga and North Kettleman fields shows a migration efficiency greater than 100 %, which is impossible unless the fetch area was formerly greater than indicated by present structure. See discussion.

One metric tonne of 30^o oil equals about 7.5 barrels.

EVALUATION OF FRONTIER EXPLORATION POTENTIAL

INTRODUCTION

The southern San Joaquin basin has three major exploration frontiers: deeper objectives along the central-basin axis, the northeastern basin flank, and the western disturbed belt. Although the charge analysis approach cannot identify particular targets in a frontier setting, it can help identify charge and trap problems which can guide prospect development and give an indication of probable overall success of an extended exploration program.

The charge analysis approach will be combined with other data to evaluate exploration potential and probable limiting factors for these three areas. The four classic trapping elements (reservoir, seal, trapping geometry, and charge) and the additional factor of timing will be evaluated for these areas to identify problems and possible settings where exploration success is likely to be more favorable.

FUTURE DEEP BASIN POTENTIAL

The stratigraphic zones of interest are the Early to Mid Miocene strata of the Maricopa and Buttonwillow depocenters and the Eocene strata of the Valley Syncline and south. The main changes in trapping elements with depth concern the reservoir quality and petroleum type. Many basin-marginal sands do not extend to the basin center. Other sands are strongly affected by burial diagenesis. At deeper depths, charge will be affected by the thermal maturity of potential source rocks. At high temperatures, charge is likely to be light oil, condensate or gas rather than the black oil characteristic of most shallow San Joaquin Basin production.

POTENTIAL RESERVOIR DISTRIBUTION

In general, early and middle Miocene sandstones thin or disappear toward the basin axis (Seiden 1964; Calloway 1990). Oligocene sandstones are absent (Seiden 1964), except in the western Maricopa and Buttonwillow depocenter (Fishburn 1990; Calloway 1990). Early - Mid Eocene sandstones are present in the northern part of the Valley Syncline, and Point of Rocks sandstones are present over the western Buttonwillow and Maricopa subbasins (Seiden 1964).

Details of sandstone distribution are beyond the scope of this study, but clearly, sandstone distribution strongly affects distribution of potential exploration targets. In the absence of sandstone targets, fractured shale and siltstone should also be considered for potential reservoirs. Fractured reservoirs without a matrix pore system have low porosity, so recoverable reserves per volume of reservoir are low.

RESERVOIR QUALITY EVOLUTION

Over 32,000 porosity and permeability core analyses were evaluated to determine controls on San Joaquin basin reservoir quality. San Joaquin rocks show declining porosity and permeability with increasing pressure and temperature. Reservoir quality was best correlated to maximum temperature, texture, and geological age. Porosity loss is associated with compaction at shallow depth and clay and zeolite cementation at higher temperature. The best quality rocks at depth are clean (shale-free) well-sorted, medium sandstones with minor fractions of volcanic fragments (shown on figure). These rocks show rapid permeability loss with increasing temperature. At high temperature, the dominant pore systems are microporous. Muddy sandstones, poorly sorted sandstones, and sandstones with substantial volcanic rock fragments have even worse porosity and permeability at high temperatures than the trends figured here. Fractured diatomites and siliciceous shales have adequate reservoir quality at shallow depths, but porosity is occluded rapidly with increasing temperature and silica diagenesis.

Most deep targets are likely to have low permeability matrix pore system regardless of the starting rock fabric, because reservoir temperature will be high. This has the following implications: (1) high viscosity fluids (black oils and light oils) will produce at low rates in the absence of fractures. Low viscosity fluids (dry and wet gases) will probably have adequate production rates. (2) transition zones are likely to be thick, because low matrix permeability is associated with high capillary-threshold pressure. (3) Pressure maintenance may be necessary for gas-condensate discoveries to prevent subsurface liquid formation and reduction in production rate. This adds to development cost.

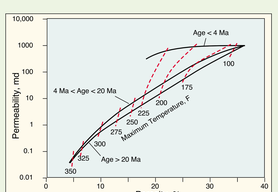

Nomograph for average porosity and permeability prediction as a function of age and maximum temperature for clean, well-sorted sandstones in the San Joaquin basin. This chart is based on empirical data. It excludes data from sandstones rich in volcanic rock fragments and calcite cement. It also excludes fracture-enhanced permeability. Observed permeability and porosity at a given temperature has a high scatter, but only a small fraction of the samples will have significantly higher porosity and permeability.

THERMAL MATURATION AND PETROLEUM TYPE

The transition from black oil generation to unassociated gas generation is typically assumed to occur at a TR of 0.9 or greater for rich marine source rocks (Pepper 1991). This corresponds to a minimum temperature of approximately 425^{0} F. based on extrapolation from the empirical TR model (Figure below). The depth at which this temperature occurs varies from about 20,00 ft at high thermal gradients to 28,000 feet at the lowest thermal gradient in San Joaquin depocenters.

The empirical transformation vs. maximum temperature trend indicates that only a small fraction of the Miocene source rock is at high enough thermal maturity for unassociated wet- or dry-gas generation. Wet-gas generation would be expected only in areas of high thermal gradient and deep burial. At low thermal gradients, depth of wet-gas formation exceeds depths of Tertiary strata in the southern San Joaquin basin.

The sparsity of gas formation predicted by this model is confirmed by the absence of thermogenic gas accumulations in deep in the basin and the common occurrence of oil and condensate staining in deep tests at temperatures exceeding 350^{0} F (e.g, Fishburn 1990), where conventional kinetic models would predict unassociated wet or dry gas formation. Even thermogenic condensate production is sparse, with major production only at Cal Canal field. This field has a gathering area with high thermal gradient and great depth of burial.

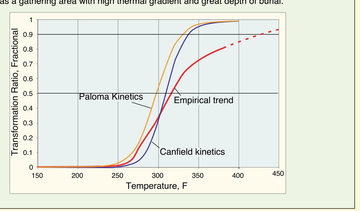

CRITERIA FOR SUCCESSFUL EXPLORATION

The two main limits are reservoir quality and petroleum type. Low matrix reservoir quality can be productive with gas, but gas is expected only in the hottest parts of the basin. With liquid petroleum, fracture networks must be present to enhance production rates. Fracture systems unsupported by matrix porosity will give good initial production, but rapid decline. This limits potential deep fracture traps to sandstone zones. Deep basin exploration should concentrate along major faults or steep dip inflections where fracturing is expected. Geopressure is insufficient for natural hydraulic fracturing except where added to the local stress field. High thermal gradient is favorable, because oil will have a lower viscosity and deep tests may encounter gas.

Expect high water saturation in pay zones and thick transition zones. High water-saturation may lead to pay recognition problems. Thick transition zones will lead to numerous shows with few economic accumulations. High petroleum column height may be necessary for water-free or low-water production. This means that structures should be high, and stratigraphic closures should include significant structural relief.

FUTURE EAST-SIDE POTENTIAL

Parts of the east side of the southern San Joaquin basin have received sufficient charge for large, economic petroleum accumulations. However, no large accumulation has yet been discovered on the east side of the basin north of the Bakersfield arch. The major exploration challenges are location of a suitable trap and location of adequate charge.

TRAP LIMITATIONS

Structural deformation is modest on the east side of the basin north of the Bakersfield arch, so the most likely trap types are stratigraphic or combination traps. Either trap type will require updip change from reservoir to seal. In the San Joaquin basin, this is most likely related to truncation of an older sandstone and deposition of a sealing facies above the truncation, or depositional pinchout of a basinal sandstone at the toe of a bypass slope. More detailed basin sandstone trap types are illustrated in Hewlett and Jordan (1993). Updip pinchout of neritic sandstones is unlikely, because shallow-marine facies are shale prone, and non-marine facies have few sealing lithologies.

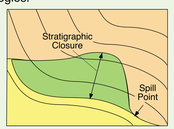

Map view of a stratigraphic pinchout trap. Solid lines are structural contours, with deepest values toward the lower left.

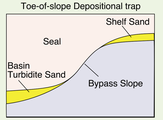

Toe-of-slope trapping is caused by depositional pinchout of a basinal sand against a bypass, shale-dominated slope.

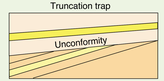

Truncation trapping is caused by a sealing unconformity with an irregular surface forming after basin-margin deformation. Uplift and erosion is followed by rapid transgression and shift to shaley outer neritic or bathyal facies. Trapping would therefore be associated with times of deformation, possibly located near major faults where differential deformation is most likely.

CHARGE LIMITATIONS

Older source horizons are thermally mature east of the Valley Syncline Axis. Much of this charge is diverted south by the north-plunging Wasco-Rio Bravo and Buttonwillow - Bowerbank axes. In the northern Valley syncline, migration is diverted north to the helm field are by a south-plunging anticlinal axis. Areas east of these axes and areas in the central Valley syncline charge to the east. Almost none o f this eastward charging oil has been discovered. This is a substantial fraction of the Eocene-sourced and Lower Miocene-sourced petroleum (Figure at right)

In the northeast area, migration patterns are broadly divergent, so large accumulations would not be expected near here, even if a trap were available. Most migration in the central eastern area is parallel, so stratigraphic focusing must be called upon to charge significant petroleum to a large trap, if one exists. .

CRITERIA FOR SUCCESSFUL EXPLORATION

The key to exploration success in this area is identifying a stratigraphic trap, because structural traps are essentially absent here. Stratigraphic trap potential is also poor. For this reason, the eastern area may be characterized by dispersed petroleum charge with little or no economic trapping.

The best truncation possibilities are truncated Mid Eocene sands trapped by Kreyenhagen seals. This is most favorable in the northern part of the east side. Charge would be from Eocene source rocks.

Toe-of-slope depositional pinchouts are most likely in Early to Mid Miocene strata. Most of this area is north of the Late Miocene Stevens-associated basin floor and submarine channel margin trapping discussed by MacPherson (1978), Webb (1981), and Hewlett and Jordan (1993). Absence of major sand source along the east flank north of the Bakersfield arch favors a shaley slope facies and updip pinchout. However, shallower bathymetry prevented deposition of Stevens and other basin-floor turbidite fans much north of the Bakersfield arch (MacPherson 1978). Best hopes are for trapping is in deeper horizons, possibly near the Olcese stratigraphic level. Alternately, if previously unrecognized younger coarse-grained sediment source are recognized north of the Bakersfield arch, then suitable trapping geometry might be recognized.

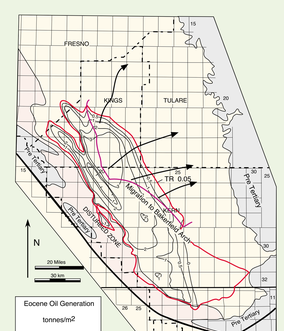

Eocene source-rock generation map, showing drainage area to east side of the basin(magenta lines) and generalized migration directions (black lines with arrowheads). Oligocene through middle Miocene drainage patterns are similar to this, but less mature source rock occurs in the area draining east.

FUTURE WEST-SIDE POTENTIAL

Most structures on the eastern side of the western deformation zone are charged, but structures farther west are incompletely charged or uncharged. Spill point elevations indicate up-plunge charge along structural axes from the SE. Most traps are combination traps, because reservoir has limited distribution on the west side.

West side frontier exploration is mainly farther west or deeper horizons. Charge and reservoir limit potential trapping. Charge limitations are caused by inadequate maturity or migration shadows from structures farther east. These structures are younger, so timing is key.

DISTRIBUTION OF MATURE SOURCE ROCK

Best source rocks (Monterey) are immature approximately west of the San Joaquin Formation onlap. Temblor rocks thicken toward the south, and deeper buried Temblor rocks are mature for oil generation on lower thrust sheets and where Temblor is buried by a thick Monterey. Monterey thins to the west, so hanging wall Temblor is thermally immature near the San Andreas Fault. Kreyenhagen rocks are thermally mature in the southern area where Temblor formation is thick, but not in the disturbed zone north of Elk Hills. Recently uplifted anticlines and thrusts bring Thermally mature formations closer to the surface.

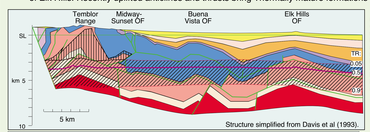

Elk Hills balanced cross section (Davis et al 1996) showing areas within the oil window thermally mature based on present temperature (diagonal hatch) and areas with uplifted thermally mature rock (vertical hatch). Eocene strata are mature along the entire section, whereas the Monterey group is entirely immature west of the San Joaquin onlap.

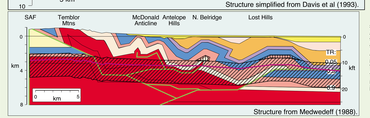

Lost Hills balanced cross section (Medweldeff 1988) showing areas within the oil window thermally mature based on present temperature (diagonal hatch) and areas with uplifted thermally mature rock (vertical hatch). Thinner Temblor and Monterey formations result in lower thermal maturity. Kreyenhagen strata are immature west of Antelope Hills.

Tulare
Paso Robles
San Joaquin
Etchegoin
S. Margarita
Reef Ridge
Monterey
Temblor
Eocene
Pre-Tertiary

Thermal maturity is estimated from TR-temperature relationship developed for cuttings in the San Joaquin depocenters. Uplifted mature zones are estimated from geohistory models constructed using sediment thicknesses interpolated from structural reconstruction. Maturity of Cretaceous rocks is underestimated because pre-Cenozoic burial was not reconstructed.

CHARGE TIMING

The greater Temblor and Monterey thickness in the SE area (near Midway-Sunset field) resulted in significantly earlier thermal maturation than rocks in the current basin depocenters. Modeled transformation initiates earlier in western wells in the Maricopa depocenter. Even earlier transformation is modeled under the easternside of the southern Temblor Range using outcrop thicknesses (Dibblee 1973). Generation starts before folding along the western margin south of Belgium Anticline. Generation started later north of Elk Hills, and Eocene strata are immature under the central Temblor Range. West-side structural growth initiated sooner in the central area as well (Harding 1976). The Belridge and Cymeric structures blocked westward petroleum migration and diverted it NW along their structural axes. This created a migration shadow west of Belgian anticline. Farther north, thin Temblor and Monterey strata are insufficient to mature Late Eocene strata for oil generation without burial by Etchegoin and San Joaquin strata. Tertiary oil generation is late or absent in the northern disturbed zone and surrounding areas. Disturbed zone fields in the Antelope Hills area are charged by generation in the syncline west of the Belridge anticline. North of the Belridge structures, there are no structures blocking migration, but Avenal Syncline generation is modest. Avenal syncline generation is Quaternary.

Modeled time of transformation of Late Eocene strata in various parts of the southern San Joaquin basin. Transformation is earliest near the eastern Temblor Range due to thick Temblor and Monterey deposition. Transformation is especially late to post-Miocene uplift. Transformation becomes progressively later toward the east due to thinner Temblor section. Although transformation near San Emidio field begins early, peak generation is later than in the central Maricopa depocenter. Similarly, this well because of reduced late Miocene and Pliocene deposition. Central Buttonwillow depocenter generation is later than central and western Maricopa depocenter generation due to thinner Temblor and Monterey sections and thicker Etchegoin and San Joaquin section.

Although Eocene strata are thermally mature in the southern Temblor Mountains, their source quality is poorly constrained and probably poor. Implications fo timing mainly apply to immediately overlying lower Temblor shales (Santos Shale). Eocene source qualit improves to the north, but its transformation is later in the Central Temblor range.

Transformation is modeled using the Lawrence Livermore kinetics. Heat flow in the eastern Temblor Mountains poorly constrained, so models with two reasonable heat flows are shown.

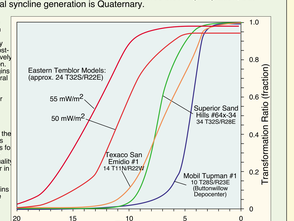

CRITERIA FOR SUCCESSFUL EXPLORATION

Western Disturbed zone exploration success depends on successful prediction of reservoir distribution (not discussed here) and charge. Overall, look for local (within disturbed zone) generation proximal to prospects or reconstruct realistic migration scenarios from kitchens farther east. Areas of generation within the disturbed zone are more likely in the southern and central areas. Timing favors effective charge in the south. Eocene and Temblor rocks are the most likely potential source rocks, but source quality needs proper assessment in the southern disturbed zone. Structural inversion north of Coalinga field makes interpretation of pre-Quaternary charge patterns to the Vallecitos and other areas difficult to assess.

CONCLUSIONS

Charge analysis of mature basins can help develop exploration concepts for nearby frontier areas. The key issues are presence of an adequate charge, timing of charge relative to structures, and migration patterns favorable for sufficient petroleum charge.

The assessment of maturely explored parts of the San Joaquin basin confirm the presence of prolific source rocks, a high expulsion efficiency consistent with earlier studies (e. g., Pepper 1991), and a high secondary migration efficiency on the order of 50 % in fetch areas with adequate traps. Overall basin trapping efficiency (reserviored oil divided by generated oil) is about 25 %, unusually high compared to the worldwide compilation of Perrodon (1995). A high degree of structural and stratigraphic focussing may help improve migration efficiency. Charge assessment using current structural configuration fails for Eocene-sourced oil in the northwestern basin due to major Quaternary structural changes.

Results were used to evaluate exploration potential in three exploration frontiers near the San Joaquin basin: Deeper targets in the central basin, east side potential, and far west side potential.

- Deeper targets in the central basin must consider the interaction between petroleum fluid type and reservoir quality evolution. Gas generation is delayed relative to oil, so the petroleum type most likely reservoired in deeper parts of the basin will be light oil and gassy condensate, not dry or wet gas. Matrix reservoir quality evolves towards a moderate porosity, low permeability network that cannot produce liquid petroleum at economic rates. This means that only the few areas of the basin with great burial and high heat flow are likely to be gas prone. Other areas require a fracture network to increase light oil production rates. Transition zones will be thick, so high stratigraphic or structural closures will be required. Overall, shows will be abundant and economic production will be localized, and likely to have a high water cut.
- Eastern margin of the basin received a petroleum charge adequate for major oil accumulations. Absence of structure and sparsity of facies changes favorable for combination trapping limit economic production. Exploration potential is limited unless a favorable stratigraphic configuration is identified.
- West side "disturbed zone" exploration west of productive marginal structures is charge and reservoir limited. Deeper potential source horizons in the southeastern area are thermally mature for oil and gas generation, but farther north, local source rocks are immature. In the central area, early structures on the east side of the disturbed zone blocked westward migration of oil, because all oil generation is after formation of the structures. Tertiary strata in the northern disturbed zone is immature for oil generation. Timing of trap formation and generation are critical exploration issues. From a charge point of view, exploration potential is better towards the south.

REFERENCES

Bishop, R. S., M. H. Gehman, and A. Young, 1983, Concepts for estimating hydrocarbon accumulation and dispersion: AAPG Bulletin, v. 67, p. 337-348.

Brown, A., 1994, Predictive vs. descriptive approaches to petroleum system concepts: presented at the First Joint PAPG/AAPG International ESRI Research Conference, Geological Aspects of the Petroleum System (October 2-6, 1994, Mexico City).

Burnham, A. K., and J. J. Sweeney, 1989, A chemical kinetic model of vitrinite maturation and reflectance: Geochimica et Cosmochimica Acta, v. 53, p. 2649-2657.

California Div. of Oil and Gas, 1985, California Oil and Gas fields, V. 1, Central California (3d. edition): California Department of Conservation, Division of Oil and Gas, Pub. TR 11, 400 pages of data sheets.

Calloway, D. C., 1990, Miocene stratigraphic nomenclature for the San Joaquin basin, California: in SEPM Pac. Sec. Pub. #64, p. 21.

Calloway, D. C., and E. W. Rennie,1991, San Joaquin Basin, California: in: H. J. Gluskoter and others, eds., Economic Geology, U.S.: Geological Society of America, p. 417-430.

Davis, J. F., S. Namson, and S. Gordon, 1996, Structure and hydrocarbon exploration in the transpressive basins of southern California: in: P. L. Abott and J. D. Cooper, eds., Field Conference Guide 1996, Pacific section AAPG, GB 73, p. 189-238.

Dibblee, T., 1973, Stratigraphy of the Southern Coast Ranges near the San Andreas Fault from Cholame to Maricopa, California: USGS PP #764, 45 p.

Drew, L. J., and J. H. Schuenemeyer, 1993, The evolution and use of discovery process models at the U. S. Geological Survey: AAPG Bulletin v. 77, p. 467-478.

Fishburn, M., 1990, Results of deep drilling, Elk Hills Field, Kern Co. California: in: Structure, Stratigraphy, and Hydrocarbon Occurrences of the San Joaquin Basin, California: Pac. Sec. SEPM pub. # 64, p. 157-168.

Harding, T., 1976, Tectonic significance and hydrocarbon trapping consequences of sequential folding synchronous with San Andreas faulting, San Joaquin Valley, California: Bull. AAPG, v. 60, p. 356-378.

Hewlett, J. S., and W. W. Jordan, 1993, Stratigraphic and combination traps within a seismic sequence framework, Maricopa depocenter, Miocene Stevens turbidites, Bakersfield Arch, California: AAPG Memoir 58, p. 135-162

Hodgson, S. F., 1980, Onshore oil & gas seeps in California: California Division of Oil & Gas, Publication no. TR06, 97 p.

Kamerling, M., R. Lewy, and L. Lundell, 1989, Biogenic origin of Pliocene dry gas, southern San Joaquin basin, California: Bull. AAPG, v. 73, p. 542-543 (Abstract).

Lundell, L. L. and S. Gordon, 1988, Origin of Cuyama basin oils: in: Tertiary tectonics and sedimentation in the Cuyama basin, San Luis Obispo, Santa Barbara, and Ventura Counties, California (W. Stanley, ed.), Pac. Sect., SEPM, pub. # 59, p. 29-37.

MacPherson, B. A., 1978, Sedimentation and trapping mechanism in the Upper Miocene Stevens Sandstone and older turbidite fans of southeastern San Joaquin Valley, California: AAPG Bulletin v. 62, p. 2243-2274.

Medwedeff, D., 1988, Structural analysis and Tectonic Significance of Late-Tertiary and Quaternary Compressive-Growth folding, San Joaquin Valley, California: Ph. D. Dissertation, Princeton University, 184 p.

Pepper, A. S., 1991, Estimating the petroleum expulsion behaviour of source rocks: a novel quantitative approach: Geological Society special publication 59, p. 9-32.

Perrodon, A., 1995, Petroleum systems and global tectonics: Journal of Petroleum Geology, v. 18, p. 471-476.

Peters, K. E., M. Pytte, T. Elam, and P. Sundararaman, 1994, Identification of petroleum systems adjacent to the San Andreas Fault, California: in: The Petroleum System--from source to trap: (Magoon and Dow, eds.): AAPG Memoir 60, p. 423-436.

Sales, J. K., 1993, Closure vs. seal capacity-- a fundamental control on the distribution of oil and gas: in: Dore, A. G. et al., eds., Basin Modelling: advances and applications: Norwegian Petroleum Society Special Publication 3, p. 399-414.

Seiden, H., 1964, Ketteman Hills Area: Selected papers presented to the San Joaquin Geological society, v. 2, p. 46-53.

Webb, G. W., 1981, Stevens and Earlier Miocene turbidite sandstones, southern San Joaquin Valley, California: Bull. AAPG, v. 65, p438-465.

ACKNOWLEDGMENTS

This work is an outgrowth of work completed at ARCO in 1995 prior to its merger with BP. I thank ARCO for permission to release these results. Jere Jay, Don Medwedeff, and Stuart Gordon provided useful comments and helped with regional tectonic and stratigraphic concepts. Mike Clarke helped with sampling for kinetics evaluation. Bob Loucks helped with compilation and analysis of reservoir quality data. Kim Touysinthiphonexay helped with evaluation of migration efficiencies. Finally, I thank Bill Bazeley who many years ago urged me to continue evaluation of San Joaquin basin charge.